Modeling of jet and pool fires and validation of the fire model in the CFD code FLACS

Natalja Pedersen

Department of Physics and Technology
University of Bergen
Bergen Norway
June 2012

Acknowledgments

This report is the result of the thesis work that I performed from August 2011 until Juni 2012 at GexCon AS. I would like to thank GexCon for giving me to do my thesis work there. Especially, I want to thank my supervisor Bjørn J.Arntzen for supervision through discussions during my work. I also want to thank my other supervisor Deiveegan Muthusamy for learning me to use CFD FLACS-Fire and Linux program and for giving me good advices, comments and support. It has been a great learning experience. I also wish to thank Bjørn Lilleberg, Idar E.Storvik and Trygve Skjold.

I want to thank my fellow students Kjetil Lien Olsen and Ingrid Anette Larsen for helping me and giving support and motivation.

And last but certainly not least I want to thank my parents, friends and boyfriend, Morten, for their deep understanding and support.

Bergen 1.June 2012

Natalja Pedersen

Department of Physics and Technology
University of Bergen
Bergen Norway

Abstract

Accidental fires can result in damage of property; endanger people, environment and lead to large economic loss. As a result, predictive estimation of properties describing fire is essential for emergency planning, control and for setting up safety mitigations.

Different scenarios of full-scale and small-scales fires can be studied by experiments or Computational Fluid Dynamics (CFD) modeling. The fires of full-scale may be difficult and very expensive to perform by experiments. The extrapolation of small-scale models to full-scale models is often unavailable. Therefore, there is need to develop computational tools capable to model both small and larger fires, where combustion process is complex.

The main focus of this thesis is to validate the fire model in FLACS code (FLame Accelerator Simulator) which is under development. The FLACS code is a 3-D Computational Fluid Dynamics code which solves the compressible conservation equations for mass, momentum, enthalpy and mixture fraction using a finite volume method. Fire simulations include such processes as buoyancy, convection, entrainment, turbulence, diffusion, combustion and thermal radiation. Therefore, the use of the following models is necessary in numerical simulations of fire: combustion models, turbulence models, radiation models, soot models and conduction in structures.

In the present work, the modeling of turbulent diffusion flames of propane jet and ethylene jet fires and heptane pool fires was performed using the FLACS-Fire code. The experiments with most relevant and available data from the literature were used for validating of the model modeling. The Eddy Dissipation Concept (EDC) was used to model the combustion. Turbulence was modeled using the $k-\varepsilon$ model. Radiation was handled using the Discrete Transfer Model (DTM). The predicted results of flame height, temperature, soot volume fractions were compared with experimental measurements and simulated results of other authors. The grid sensitivity and parametric analysis were performed in simulations of jet fires. The finest grid size was equal to the one leak cell within the flame domain. Outside the flame domain the grid was stretched towards the boundaries. The changes in such parameters as time step length, turbulence length scale and number of rays in radiation model were tested in simulations of basic case which represented the best predicted results.

The predicted results of temperature in ethylene jet fire with finest grid resolution were in good agreement with experimental measurements. The results of temperature were strongly influenced by changes in relative turbulence intensity in the jets. The importance of radiation was tested and showed that the predicted temperatures were significant dependent on radiation modeling. The flame heights were over-predicted for all propane jet flames. FLACS-Fire was unable to predict lift-off distance which could have influence on prediction of the flame height. The prediction of soot volume fractions was reasonable in comparison to experimental measurements.

The simulations of heptane pool fires showed that the FLACS-Fire was able to model pool fires. The predicted temperatures at the centerline of flame were over-predicted comparing to experimental measurements. The modeling of pool fire using FLACS-Fire gave very rough approximation to the real pool flame. The consideration of buoyancy and heat feedback effect in the numerical simulations is necessary for reasonable modeling of pool flame.

Latin letters

Symbol	Description
$C_\mu, C_{\varepsilon 1}, C_{\varepsilon 2}$	constants in the *k*-ε model
$\dot{Q}_c$	total heat release rate
$\dot{m}''$	mass burning rate
h_i^o	specific enthalpy of formation of species *i*
A_f	surface area of the fuel
A_o	preexponential factor
E_a	activation energy
H_F	flame height
L_V	evaporation heat of fuel
P_k	production rate of *k*
R_u	=8.314kJ/kmolK; universal gas constant
S_i	source term of species *i*
X_i	mol fraction of species *i*
Y_i	mass fraction of species *i*
Z_i	element mass fraction of species *i*
$c_{p,i}$	constant pressure specific heat capacity
k_f	specific reaction rate coefficient
l'	turbulent length scale
l^*	fine length scale
m_i	mass of species *i*
m_{tot}	mass for all species
u',	turbulent velocity scale
u^*	fine velocity scale
x_i	cartesian coordinates, *i*=1, 2, 3
ΔH_c	heat of combustion
D, d	diameter
E	radiation emissive power
Fr	Froude number
g	gravity acceleration
h	specific enthalpy
h	convective heat transfer coefficient
k	turbulence kinetic energy
M	molecular weight of mixture
p	pressure
r	stoichiometric coefficient
R	reaction rate
Re	Reynolds number
T	temperature
t	time
u	velocity
x	distance
$\dot{Q}, \dot{q}$	heat flux
k	thermal conductivity
C	concentration
$\Delta H_{f,r}$, $\Delta H_{f,p}$	enthalpy change for reactants and products at standard state

Greek letters

Γ_i	diffusion coefficient
Φ_i	scalar variable
k_f	specific reaction rate constant
μ_t	dynamic turbulence viscosity
$\sigma_k, \sigma_\varepsilon$	turbulence Prandtl-Schmidt number in k and ε equation
τ^*	turbulence fine structure time, residence time
τ_c	chemical time scale
n	number of mol
x	combustion efficiency
β	configuration factor
ε	dissipation rate of k
μ	dynamic viscosity
ν	$=\mu/\rho$ kinemiatic viscosity
ξ	mixture fraction
ρ	density
σ	$=5.67 \times 10^{-8}$ W/m^{2}K^4 Stefan- Boltzmann constant
τ	turbulent time scale
χ	fractions of reacting turbulence fine structures
ϵ	emissivity
ϕ	equivalence ratio

Subscripts

conv	convection
L	losses
rad	radiation
cond	conduction
F	flame
f	fuel
t	turbulence
ox	oxygen
LFL	lower flammability level
LFU	upper flammability level

Superscripts

´´	fluctuating value
-	mean
~	mass weighted
*	fine structure state
°	surrounding fluid state

Contents

1 Introduction

Accidents are associated with the occurrence of fires, explosions or atmospheric dispersions of hazardous materials. They can involve more than one of these phenomena: a fire can cause the explosion of a vessel, an explosion can be followed by fire, and an explosion can cause a dispersion of a toxic cloud. These accidents can affect people, property and the environment. Following the historical analysis, the increase of accidents occurred in the process industry due to significant development of the processing industries during the last few decades. The survey of accidents in the process plants and in the transportation of flammable materials distribution is shown in Figure 1-1 [1].

	Number of accidents	% of total
Known type of accident	5921	96.0
Unknown type of accident	247	4.0
	Number of accidents	**% of known types**
Loss of containment	3022	51.0
Fire	2603	44.0
Explosion	2133	36.0
Gas cloud	719	12.1

Figure 1-1 *Historical analysis of accidents [1]*

The accidents based on four different types: release, fire, explosion and gas cloud. The figure shows the distribution of events. Two types could exist in each accident. A release occurs in more than 50%, the fire is the most frequent accident (44%) of the three hazards (fire, explosion and gas cloud). There are several types of fire: pool fire, jet fire, flash fire, fireballs [2]. The generation of each depends on different conditions. For example, a pool fire occurs when a flammable liquid spills into the ground and is ignited. Pool fire may also occur on the surface of pool spilled on water. Jet fires typically result from gas releases from high pressure equipment. Combustion involves turbulent fluid flow, chemical reactions, heat transfer and other complex physical and chemical processes. There are number of experimental and numerical studies of fires.

CFD (Computational Fluid Dynamics) is software that solves the three-dimensional Navier-Stokes equations (governing equations) for compressible or incompressible flow by numerical methods. In 1970, the possibilities of CFD were limited to two–dimensional flows [3]. Today, the digital computers have sufficient storage and speed capacity to allow CFD to solve the fluid flow in real three- dimensional world. CFD is an increasingly used tool to investigate the behavior of fire and predict the consequences of fire hazards. There are several software packages for CFD modeling related to fire for example, Fire Dynamics Simulator (FDS) [4], Kameleon FireEx [5] and CFX [6].

1.1 Motivation

CFD software is used in calculating of many engineering applications. Development of them is important for predictions of risk in the process industry. Risk of an accident leak and its ignition might results in a fire with potential hazards on humans, property and environment. The fire modeling using CFD is an attractive alternative to experiments and empirical correlations. Numerical simulations help to perform experimental investigations of large-scale fire phenomena that can be expensive and extrapolation from experimental results is usually not possible for safety studies.

The turbulent combustion modeling is a broad subject where estimation of fluid mechanical properties, chemical reaction rates, radiative transfer heat is domain of interest. Computer simulations of fire help to calculate the different characteristics of fire in time and space: temperature, heat fluxes, the thermal radiation intensity, smoke emission, production of certain toxic gas species and etc. It is very important to perform validation analysis to ensure accuracy of the results. Validation of numerical codes and models are necessary first step before their application in risk assessment analysis.

The FLACS–Fire code is CFD tool for modeling quantitative risk assessment related to fire hazards in the process industry. The model must be developed and validated before FLACS-Fire can be used with confidence for describing large-scale fires in industry. Aim is to be the best validated fire-code on the market.

1.2 Objective

The objective of this work was to perform validation of FLACS-Fire, which describes the complex interaction between turbulent flow, convection, non-premixed combustion, air entrainment, buoyancy, soot formation, thermal radiation, toxic combustion products and dispersion of smoke. Validation is an iterative process of comparing the model to actual system behavior and using the discrepancies between two for to improve the model. This process is repeated until model accuracy is judged to be acceptable.

In the present work, the modeling of turbulent diffusion jet and pool fires was used to validate FLACS-Fire code. Simulations of jet and pool fires were based on experimental work. Predicted results of temperature, flame height, soot volume fractions were compared to experimental measurements and numerical results of other research groups. A comparison between the simulations results and experimental measurements were used in order to assess the accuracy of the model and suggest its improvements.

In modeling of jet fires, the simulations were performed with different grid resolution. Influence of such parameters as Courant-Friedrich-Levy number based on speed on sound (CFLC), Relative Turbulence Intensity (RTI), Turbulence Length Scale (TLS) and number of rays in radiation model (RADMODD) was tested by performing simulations with changed value of parameter. Importance of radiation model was tested by to perform simulation without radiation model.

1.3 Overview of thesis

A theoretical background of the combustion process, with focus on jet fire flames and pool fires, is given in Chapter 2. Chapter 3 presents the physical fundamentals of fire modeling. This includes brief introduction of the CFD code FLACS-Fire used for all calculations in the present work. In Chapter 4, a literature search of existing work is presented. Chapter 5 deals with modeling of experimental turbulent diffusion flames of jet and pool fires using FLACS-Fire. Chapter 6 presents results from simulations of turbulent diffusion flames of jet and pool fires. Predicted values of temperature, soot volume fractions, flame height are compared with measurements and simulations of other authors. For ethylene jet flame, effects of grid resolution and changed parameters are studied. In additional, the importance of radiation model is tested. The difference between predicted and experimental results are shown and discussed. In chapter 7 conclusions are given. Recommendations for further work are described in Chapter 8.

2 The combustion process

This chapter is an introduction to the fire dynamics. Combustion process of different fuels, necessary factors for fire and detailed mechanism of heat transfer by convection, conduction and radiation are presented.

2.1 Combustion of fuels

Combustion is the rapid oxidation of fuel in which heat and usually flame are produced [7]. The combustion fuels can be gases, liquids or solids. The burning of them occur when flammable fuel in combination with a sufficient quantity of an oxidizer such as oxygen in the air is exposed to an ignition source with significant amount of energy for to start ignition of fuel /oxygen mix. Most of ignited fuels will give a visible flame. Flame is a light given off by burning gasses during combustion process. Fire involves many chain reactions. The fire tetrahedron is a simple model for presentation of four necessary factors for fires. Figure 2-1illustrates a fire requires four elements: heat, fuel, an oxidizing agent and chain reaction.

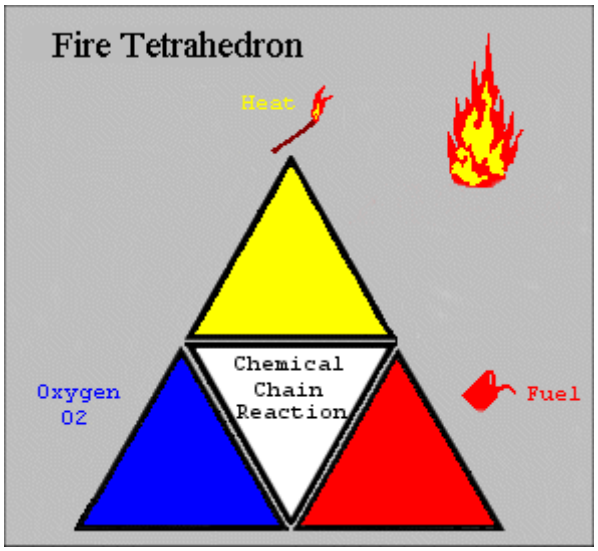

Figure 2-1 *Fire tetrahedron [8]*

Combustion fuels such as solids and liquids require the conversation of them to gaseous form. Liquid fuels are heated until they begun to evaporate and the vapor mix with oxidizer, and ignites. Burning of solids requires much more energy than simple evaporation. Evaporation of low molecular weight molecules from solids surface occurs by pyrolysis process (chemical decomposition) where the surface temperature of burning solids is high.

Oxidizer is other reactant of the chemical reaction. In the most cases, it is oxygen from the ambient air reacts with fuel. The chemical reaction is supplied by incoming oxygen (approximately 21 % in the air). Oxygen should be mixed with fuel in certain proportional before ignition (premixed flames) or oxygen diffuses into the combustion zone by force due pressure and density differences between the fire region and surrounding air. Under

combustion process is produced energy of different amount. It should be enough energy to maintain the evaporation of the volatiles from the fuels surface and suppose combustion.

Each combustion fuel has flammable limits and can only be ignited in range between lowest LFL and highest UFL concentrations of its vapor in air and sufficient temperature must exist in this region.

Chemical reaction is an oxidation process of fuel by oxidizer (air). The chemical reaction can be described by the chemical equation as

$$Fuel + r\ Oxidizer \rightarrow (1 + r)Product \qquad \textbf{Eq. (2.1)}$$

where the r is stoichiometric coefficient. The stoichiometric coefficient represents the ratio between fuel and oxidizer that can be based on mass of fuel and oxidizer or number of moles.

The combustion process is a chain reaction process involving a large number of single, elementary reactions [9]. For example, the simplest hydrocarbon, methane, includes over 40 different chemical reactions. The combustion is sustained by formation of radicals. Every elementary reaction can be characterized by chemical reaction rate. Detailed description of chemical reaction rate is given in Section 3.5

Combustion process can be complete or incomplete. In a complete combustion reaction the fuel reacts completely with sufficient amount of oxidizer (oxygen) to only such products as carbon dioxide (CO_2) and water (H_2O). There are no by-products such as carbon monoxide (CO), hydrogen (H_2), nitrogen oxide (NO) and soot (mostly C). In actual fires combustion reaction is incomplete.

Complete chemical reaction is one where all reactants is used up and converted into products. A useful parameter to describe the state of the reactant mixture (concentrations) is the equivalence ratio ϕ as defined by the following dimensionless relationship

$$\phi = \frac{(fuel/oxidizer)_{actual}}{(fuel/oxidizer)_{stoichiometric}} \qquad \textbf{Eq. (2.2)}$$

where ϕ is equal to 1 for a stoichiometric mixture. If $\phi > 1$ the mixture is reach and if $\phi < 1$ the mixture is lean.

In combustion, the description of reacting gas mixtures is mainly interested. For a mixture of different species, the distribution of species in the mixture can be describe by mass fraction of species i

$$Y_i = \frac{m_i}{m_{tot}} \qquad \textbf{Eq. (2.3)}$$

where m_{tot} is the sum of the mass for all species in the mixture and m_i is the mass related to individual species i.

In analogy to the mass fraction of species, the mixture fraction can be used in analysis of non-premixed combustion to describe the degree of scalar mixing between fuel and oxidant. The mixture fraction can be written in terms of element mass fraction [9] as

$$\xi = \frac{Z_i - Z_{i.ox}}{Z_{i,f} - Z_{i,ox}} \qquad \textbf{Eq. (2.4)}$$

Where Z_i is the element mass fraction, Z_{i1} is the element mass fraction to flow 1 (fuel) and Z_{i2} is the element mass fraction to flow 2 (oxygen). Element mass fraction Z_i denotes the ratio between the mass of an element i and the total mass. The diffusion coefficients are equal for all species in turbulent flow. The element mass fractions cannot be changed by chemical reaction. They are changed by mixing process.

For the mixture gases in combustion processes of flames, the mixture gases can be assumed to behave as an ideal-gas mixture. The temperature, density and pressure of the mixture are related by the ideal-gas equation of state [9]

$$p = \rho \frac{R_u}{\bar{M}} T \qquad \textbf{Eq. (2.5)}$$

where ρ is the density (kg/m^3), p is the pressure (Pa), T is the absolute temperature (K), R_u is the universal gas constant (8.314 J/Kmol) and $\bar{M}$ is the mean molecular weight of a mixture (g/mol).

The mean molecular weight of the mixture can be calculated as

$$M = \sum_{i=1}^{n_s} X_i M_i \qquad \textbf{Eq. (2.6)}$$

where $X_i$is the mol fraction of species i. M_i is molecular weight of species i.

The enthalpy for an ideal-gas mixture can be described by

$$h = \sum_{i=1}^{n_s} Y_i h_i \qquad \textbf{Eq. (2.7)}$$

where $Y_i$is the mass fraction of species i and h_i is function of temperature

$$h_i(T) = h_i^o + \int_{T^o}^{T} C_{p,i}(T)\partial T \qquad \textbf{Eq. (2.8)}$$

where h_i^o is the specific enthalpy at formation at given temperature, and $C_{p,i}(T)$ is the specific heat capacity at constant pressure.

2.2 Heat transfer

An understanding of fluid dynamics, mass and heat transfer is required in order to study fire phenomena. The fundamentals of heat transfer will be reviewed in this section. The heat transfer is classified into three basic mechanisms: conduction, convection and thermal radiation. Physical laws describe the behavior and characteristics of each of them. A real system of fires may include all three mechanisms. In a large fire usually radiation predominates.

Conduction is the heat transfer through the material from a region of higher temperature to a region of lower temperature. This flow can be expressed as a heat flux in one direction, which is given by Fourier's low:

$$\dot{q}_{cond} = -k\frac{\Delta T}{\Delta x} \quad \left[\frac{W}{m^2}\right] \qquad \textbf{Eq.(2.9)}$$

where ΔT is the difference in temperature (K) over a distance Δx (m) , that the heat is transferred. The constant *k* is the thermal conductivity with units of W/mK and dependent on temperature. On a microscopic scale, conduction heat transport occurs by hot and rapidly vibrating of atoms and molecules that interact with neighboring atoms and molecules and transfer some of their energy to neighboring molecules. Conduction heat transfer may occur under steady or unsteady conditions. Under steady-state conduction the temperature within the system does not change with time. Conversely, the under unsteady conduction the temperature within system vary with time. In fires the temperature in solids change with time. Analysis of unsteady heat conduction determines by approximation theories or numerical calculations.

Convection is the heat transfer by the movement of a gas or liquid from hot surface to its surroundings. Convection heat transfer occurs at all stages in a fire. Convection is important in the early stage of combustion process when thermal radiation level is low. A free or natural convection is a self-sustained flow driven from buoyancy forces created by density differences, and the density differences are caused by temperature gradients in the fluid. Buoyancy forces influences the shape and behavior of the flame. Forced convection is heat transfer in which fluid motions is generated by an external source like a pump device and the flow is independent of density differences. Buoyancy forces also exist, but usually they have only a small effect. Convection heat transfer can be described by empirical relationship by Newton:

$$\dot{q}_{conv} = h\Delta T\left[\frac{W}{m^2}\right] \qquad \textbf{Eq. (2.10)}$$

Where $\Delta T\ (K)$ is the temperature difference between the hot and cold medium. For example hot smoke and wall or hot wall and surroundings cold air. *h* (W/m^2K) is the convective heat transfer coefficient and depends on the characteristic of the system, the geometry of the solid, the properties and parameters of the fluid. One of the major problems in the heat transfer was evaluation of *h* for different situations.

Radiation is the heat transfer through space by electromagnetic waves confined to a relatively narrow "window" in the electromagnetic spectrum. Figure 2-2 illustrates the electromagnetic spectrum of different wavelength.

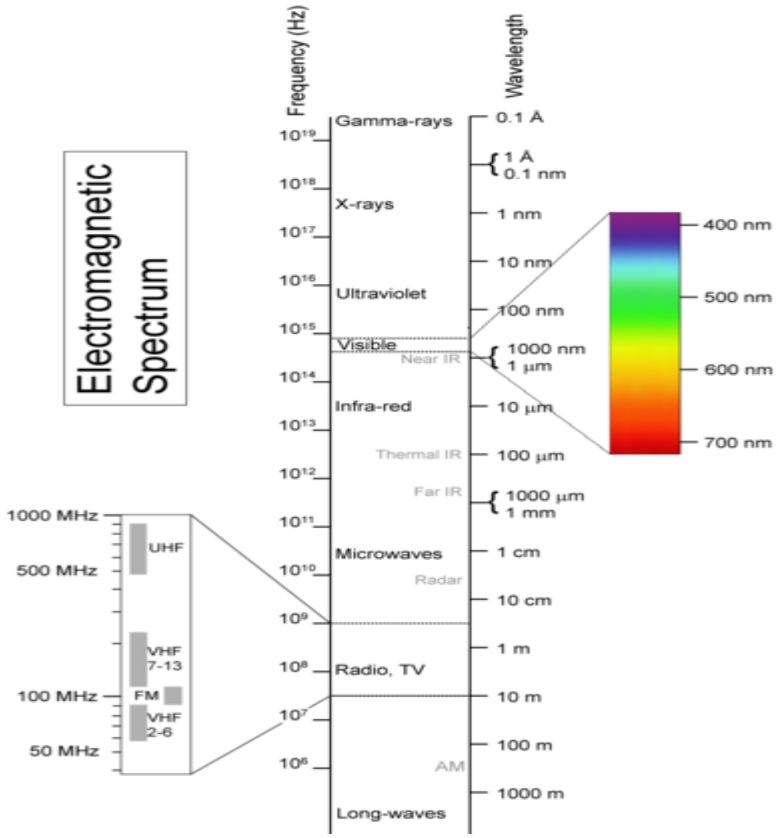

Figure 2-2 *Electromagnetic spectrum [10]*

Thermal radiation lies in the range from 0.1 µm to 100 µm, which incorporates visible-light and extends towards the infrared regions. The visible-light portion of the spectrum is from 0.35 µm to 0.75 µm. Radiation can be absorbed, transmitted or reflected at a surface in all parts of the electromagnetic spectrum. Convection predominates at low temperatures (< 150℃-200℃) but above 400℃ radiation becomes dominant. In a large scale fires where the fuel diameter increases above about 0.3m radiation usually dominates. The contact between heat source and receiver is not required for transfer of heat by radiation. Objects is located away from the fire can be heated up and auto ignites after some time. Radiation heat transfer can be described by so-called "black-body", which is defined as an idealized physical body that absorbs all incident electromagnetic radiation that falls on its surface. The total radiation energy (emissive power) emitted by a black body is proportional to T^4, where T is absolute temperature (K) and can be expressed with Stefan-Boltzmann law as:

$$E = \epsilon\sigma T^4 \ \ [W/m^2] \qquad \textbf{Eq. (2.11)}$$

where σ is Stefan-Boltzmann constant (5.67×10^{-8} W/m^2K^4) and ϵ is the efficiency of the surface as a radiator, called emissivity. The black body is perfect emitter and has en emissivity equal one. Taking into account the geometrical relationship between the emitter and the receiver, the radiation can be calculated by inserting the configuration factor β as

$$\dot{q}_{rad} = \beta\epsilon\sigma T^4 \ [W/m^2] \qquad \textbf{Eq. (2.12)}$$

2.3 Flame behavior

Combustion process is based on mixing between fuel and oxidizer and fluid motion. There are a several categories of flames. The Table 2-1 shows examples of them.

Premixed flame is a flame where the fuel and oxidizer is mixed before burning. Non-premixed flame (diffusion flame) is a flame in which the fuel and oxidizer is mixed and burned simultaneously by diffusion. Each of these combustion regimes is further divided into laminar and turbulent flow motion. The laminar flames are characterized by low flow rates in contrast to turbulent flame. The Reynolds number is often used to determine the flow regime. The Reynolds number, *Re* is a dimensionless number defined as the ratio of inertia forces to viscous forces [9]

$$Re = \frac{\rho u D}{\mu} = \frac{uD}{\nu} = \frac{inertia\ forces}{viscous\ forces} \qquad \textbf{Eq. (2.13)}$$

Where ρ is the density (kg/m^3) of the fluid, u is the velocity (m/s), D is the release diameter (m) and μ is the dynamic viscosity (kg/ms) and ν is the kinematic viscosity (m^2/s).

For low Reynolds number fluid motion is steady and smooth and flow said to be laminar. Transition stage will be reached with increasing the Reynolds number. At high Reynolds number flow will be turbulent containing vortices or eddies in very large spectrum of size. This will be further discussed in the chapter on combustion modeling, Section 3.5.

Table 2-1 *Example of combustion systems based on mixing of fuel and oxidizer and flow motion [9]*

Fuel/Oxidizer Mixing	**Fluid Motion**	**Examples**
Non-premixed (diffusion)	Laminar	Candle flame, small pool fire/jet fire
	Turbulent	Aircraft turbine, diesel engine, pool fire, jet fire
Premixed	Laminar	Bunsen flame, flat flame
	Turbulent	Gasoline engine, gas explosion

Non-premixed flames are typical for fires. The fuels come from a source like jet, pool or a solid material, and mixed with the air supported from outside. The flame is controlled by mixing process of fuel and air. Most fires are turbulent diffusion flames.

2.4 Introduction to the turbulent diffusion flames

In this section, the description of turbulent non-premixed flames such as jet flame and pool fire is presented. The type of flame can be determined by Froude number, *Fr* which shows the strength of momentum and buoyancy in fire and expressed as

$$Fr = \frac{u^2}{gD} \qquad \textbf{Eq. (2.14)}$$

where u is the velocity of the gases (m/s), D is the diameter of the burner (m) and g is the acceleration due gravity (m^2/s). Turbulent jet flames have high Froude number and the flames are dominated by the momentum. In pool fires, the flow is usually buoyancy dominated with a Froude number below 1.0 [7].

The turbulent non-premixed flames are of interest in many applications, for example diesel engines, rocket engines, gas turbines boiler furnaces, flares in rafineries/ oil fields. For any particular application, the combustion intensity and efficiency, flame stability, heat transport pollutant emissions, flame height and size are most important properties in designer and in order to produce the safety. It is necessary to know the effects of thermal radiation and soot/products concentration on structure, humans and environment. Fire hazards can be characterized in terms of heat transfer during combustion which can determine by heat release rate, the flame spread rate, the radiation to the surroundings.

2.4.1 Jet fire

A jet fire is a specific type of fire that occurs when a high-velocity fuel leak flow is ignited. The turbulent jet fires are typically characterized by as high pressure release of gas from limited size openings from pipe, flange, tank or valve. The discharge release rate of flow is dependent on the pressure inside the equipment, the hole size and shape, and the molecular weight of the gas.

The vertical turbulent jet flame form is dominated by the momentum of the release and has a cylindrical form [7]. Parameters that can influence the flame shape are the wind speed, the material properties, the conditions of the material and atmospheric conditions.

In laminar regime, the flame height of jet fire will increase with increasing of jet velocity. Above the certain velocity, the turbulence begins at the flame top and extends further down towards the burner nozzle with increase of velocity. The flame height decreases with increasing of flow velocity in turbulent regime. When the flame is fully turbulent, the flame height will reach constant value. Figure 2-3 illustrates the transition of the jet flame regime and the flame length with increasing jet velocity.

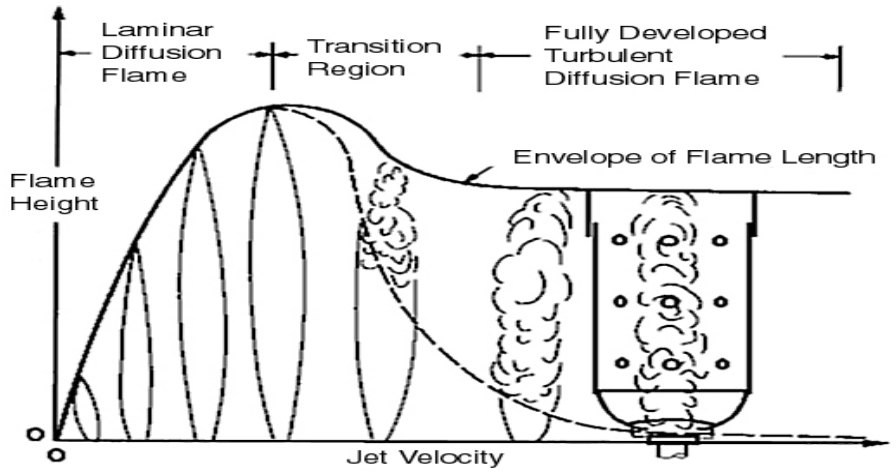

Figure 2-3 *Height of momentum jet flames as a function of nozzle velocity, showing transition to turbulence [11]*

Jet flames of high velocity are usually lifted where the base of jet flame is not attached to the release source due to the high velocity and richness of the fuel near the heat source. The distance between the jet exit and the beginning of the flame is called lift-off distance.

2.4.2 Pool fire

A pool fire is defined as a turbulent diffusion fire burning above a horizontal pool of vaporizing hydrocarbon fuel. Pool fires are buoyantly controlled gas burners. The flame of pool fire can be divided into three distinct zones: a "continuous flame zone", an "intermittent flame zone" and a "plume zone" [12]. The continuous zone presents a visible flame just above the burner and temperature and temperature remains constant. The intermittent zone is characterizes by intermittent flame pockets and corresponds to region above the continuous zone. The temperature decreased with distance from the burner. The plume zone is not visible flame where the temperature continues to drop.

The initial velocity of the evaporation in the pool fires cannot be measures, but can be derived from the rate of heat release.

The total heat release rate (HRR) is amount of energy produced by the flame per unit time. The HRR is the driving force for fire. The heat release is not a fundamental property of a fuel and therefore, cannot be calculated from the basic material properties. This parameter usually is determined from testing. The most common method to measure HRR is oxygen consumption calorimeter. Another method for determination of HRR is based on the measurements of burning rates, which is known as the mass loss rate. When the fuel burns the mass loss of fuel is weighted using weighting devices. The simplest form of HRR can be expressed as [7]

$$\dot{Q}_c = A_f \cdot \dot{m}'' \cdot x \cdot \Delta H_c [kW] \qquad \textbf{Eq. (2.15)}$$

where A_f is the surface area of the fuel (m^2), $\dot{m}''$ is the mass burning rate or mass loss rate/vaporization rate (kg/s), ΔH_c is the heat of combustion of the volatiles (kJ/g), x is an efficiency factor that takes into account incomplete combustion. (Efficiency factor depends on the fuel type, soot production, ventilation conditions and flame size).

The complete heat of combustion is the total amount of heat released when unit quantity of fuel is oxidized completely, leaving no residual of fuel and releasing all of the chemical energy of the material, $x \sim 1$. Heat of combustion is normally determined at constant volume in a "bomb" calorimeter where a known mass of fuel is burnt completely in an atmosphere of pure oxygen. The total heat of combustion can be calculated from heat of formation for all reactants ($\Delta H_{f,p}$) and products ($\Delta H_{f,r}$) in the chemical reaction. Heat of formation defined as the enthalpy change when compound is formed in its standard state (pressure 1atm and temperature 298K) from its constituent elements and their standard states[7].

$$\Delta H_c = \frac{\sum \Delta H_{f,p} - \sum \Delta H_{f,r}}{n_f} [kJ/mol] \qquad \textbf{Eq. (2.16)}$$

The mass burning rate is the mass of fuel supplied to the flame per second, per unit area of the pool. This parameter is the most important input value in numerically investigations of pool flames. The mass burning rate is dependent of the rate of heat transfer from the flame to the fuel surface. The rate of burning can be expressed as

$$\dot{m}'' = \frac{\dot{Q}_F - \dot{Q}_L}{L_V} [kg/s] \qquad \textbf{Eq. (2.17)}$$

Where $\dot{Q}_F$ is the heat flux supplied from the flame (kW/m^2) related to the energy release rate within the flame by three mechanisms of heat transfer (sum of heat transfer by radiation, conduction and convection). $\dot{Q}_L$ is the losses of heat flux through the fuel surface (kW/m^2) and L_V is the heat required to produce the volatiles (kJ/kg), which for liquid fuel is the evaporation heat. The rate of fuel evaporation depends on the rate of heat feedback from the flame to the fuel surface and the mass evaporation rate controls the total heat release rate and the rate of heat feedback. The burning rate plays a significant role in fires because it represents how much energy release into system.

The heat transfer mechanisms from the flame to the fuel surface are changed with pool diameter. When pool diameter is very small, convective heat transfer determines the burning rate while radiation heat transfer predominates in fires with large diameter. The heat conduction through the rim of the pool container has minimum contribution in pool fire.

Reported in the book of Drysdale [7], Blinov and Khudiakov (1957) studied the burning rates of different liquid pools with diameter from 3.7×10^{-3} to 22.9m. They found that the rate of burning expressed as a regression rate R (mm/min) (equivalent to the volumetric loss of liquid per unit surface area of the pool in unit time) was high for small-scale pools (1cm diameter and less) and exhibited a minimum around 0.1m diameter. The regression rate depends of pool diameter and distinguished in three regimes. If the diameter is less than 0.03m, the flame is laminar and burning rate and regression rate falls with increase in diameter. If diameter is large (D >1m), the flames are fully turbulent and burnings rate becomes independent of diameter. Flame has transitional behavior, between laminar and turbulent in the range 0.03 < D < 1.0m.

Flame height

The height of flame is an important quantitative characteristic of fire that needs to be considered in fire safety design. Flame height may affect fire detection, suppression system, building structures, smoke filling rates, fire ventilation and escape possibilities. The flaming regions above the fuel source of pool fires fluctuate periodically so that the tip of the flame is significantly different from the length of the continuous combustion. The flame height has

been defined by various criteria in order to correlate data. The height of flame depends on two variables: the heat release rate and diameter. The correlation of Heskestad is widely used to determine the flame height of pool fires with no cross-wind [7]

$$H_F = 0{,}23\dot{Q}_c^{2/5} - 1{,}02D\ [m] \qquad \textbf{Eq. (2.18)}$$

where D is the pool diameter (m) and $\dot{Q}_c$ is the total rate of heat release (kW).

Flame temperature

Flame temperature depends on many factors such as:

- Whether the fuel flow is laminar or turbulent
- Whether the fuel and oxidizer are premixed or diffuse before burning.
- Whether the flame is adiabatic (meaning does not lose heat)
- In the diffusion flames, the flame zone is heterogeneous. This gives variations in temperatures depending on the position in the flame.
- For flames in air, the temperature, pressure humidity, present gas mixture of the air.
- The higher emissivity value gives lower flame temperature due to larger radiation heat loss.

The combustion zone of diffusion flames is very narrow and has highest temperature. The regions of the flame that are away from the combustion zone have lower temperatures. Turbulent mixing of fuel and oxygen leads to pulsing behavior of the flame which affects the flame temperature.

Radiation

There are large differences in the radiative emission characteristics of fires depending on the fuel composition. Heavier hydrocarbon flames produce high concentrations of soot. In contrast, methanol burns cleanly with no soot. Hydrocarbon fires are extremely luminous due to significant concentrations of soot particles which emit blackbody radiation. Gas species such as carbon dioxide, water and carbon monoxide and hydrocarbon intermediates emit infrared radiation. Visible intensity of radiation is emitted by soot. In the large fires, the heat feedback mechanism is dominated. Feedback is the radiative transfer from the flame to the fuel surface that controls the fuel mass evaporation rate.

3 Fire modeling

This chapter focuses on computational fire modeling. A fire is a complex phenomenon to understand and model. There are an enormous number of possible fire scenarios where computation power and physical insight for all the necessary calculations are limited. The methods for studying of different fire scenarios are simplified by idealized descriptions and approximate solutions for real fire system. The methods for analysis should be improved as computing power and physical insight increase. Fire modeling can be divided into two categories, zone model and field model (CFD model) [13].

The zone model is practical for modeling fire process in enclosure. The zone model assumes that the burn room is divided into two layers (the upper layer of hot gases and the bottom layer of cold gases).

The field model divides the computational domain into a three-dimensional mesh includes of many small cells in which the fluid flow and heat transfer parameters are resolved. The physical changes in each cell are calculated by using the fundamental equations of fluid dynamics. The objectives of this chapter are the presentation of the fundamental equations in fire modeling and overview of used models in fire processes: turbulent models, combustion models, radiation models and soot models.

3.1 Field modeling

Field modeling of the fire dynamics includes two components: the CFD Methodology and the Fire Model. Figure 3-1 Illustrates the modified field modeling [13]. The CFD is represented with the fundamental governing equations of the fluid dynamics. This is the set of transport equation for mass, momentum, enthalpy and mass fraction of species and mixture fraction. Fire modeling contains the detailed specification of the fire description such as combustion, radiation and soot production.

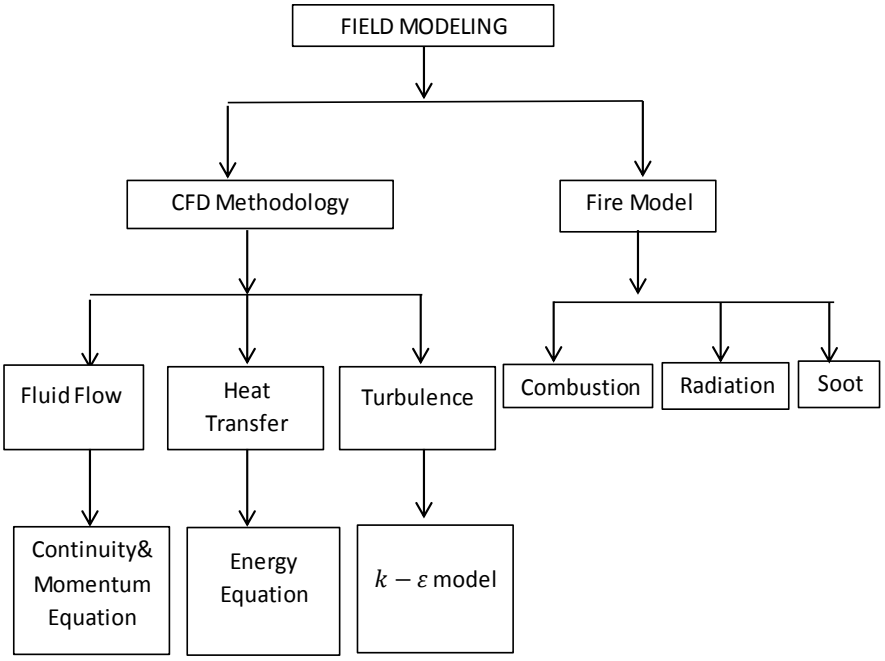

Figure 3-1 *Field modeling [13]*

The experimental investigation and numerical simulations have been used to study the fire dynamics for to improve understanding of combustion processes and allow approach for fires safety risk assessment. An experimental investigation involving full-scale equipment test can be expensive and often impossible. The small-scale models do not always give all the features of the full-scale equipment. There are many difficulties to of measurements in many situations and instruments are not free from errors.

Fortunately, the development of numerical methods and the availability of a large digital computers help to work out the implications of a mathematical model for almost any practical engineering problem. High speed computer can resolve complex fluid dynamics issues with the lowering cost and greater speeds. A computer solution of a problem gives detailed and complete information of all the relevant variables such as velocity, pressure, temperature, concentration, turbulence throughout the domain of interest. Computer analysis depends on both the mathematical model and numerical methods. Combination of correct numerical method and an adequate model are very important significant for good results. CFD is a powerful and useful tool in many industries for example aeronautics and astronautics, automotive, mechanical, chemical, electrical electronic and environmental engineering.

Both the experimental and numerical methods for investigation of fires have strengths and weakness. An optimal prediction effort should include combination of computation and experiment. An experimental method is prototype testing for the validation of CFD models. The proportions of the two methods would depend on the nature of the problem, on the objectives of the prediction, and on the economic and other constraints of the situation.

3.2 FLACS code

This chapter presents the general information about the CFD tool FLACS, following the basic framework of FLACS user´s manual [14].

The FLACS code (Flame Accelerator Simulator) is a 3-D Computational Fluid Dynamics code. FLACS has been developed since the 1980s by Christian Michelsen Institute (CMI), Christian Michelsen Research (CMR) and currently GexCon since 1980. The first version of FLACS code was released in 1986. FLACS version 9.0 was the first version that was run under both the Linux and Windows operating systems and includes the FLACS-fire test. FLACS solves the compressible conservation equations for mass, momentum, enthalpy, mass fraction of species and mixture fraction on a 3D Cartesian grid using a finite volume method (control-volume-based technique) to convert the governing equations to algebraic equations. FLACS software is especially used to simulate process safety applications such as:

- Gas and dust explosions
- Dispersion of flammable or toxic gases
- Propagation of blast and shock waves
- Pool and jet fires are under development

CFD software FLACS consists a pre-processor (CASD), a post-processor (FLOWVIS), CFD simulator and utility programs in FLACS.
The pre-processor CASD is used to prepare input data that defines a FLACS simulation scenario including geometry, computational grid definition, gas composition, size and location of leakage, ignition location and output values. A solver calculates the scenario. The post-processor FLOVWIS is a program for visualizing results such as temperature, pressure and radiation in 2D/3D plots, monitor points and simple line plots.
FLACS has primarily been developed to model dispersion and explosion phenomena. However, models for the simulation of fires are under development where the aim is to handle industrial fires of large and complex geometries. FLACS-Fire can be used as tool to study fundamental fire dynamics.

Models included in FLACS-Fire are presented in Figure 3-2.

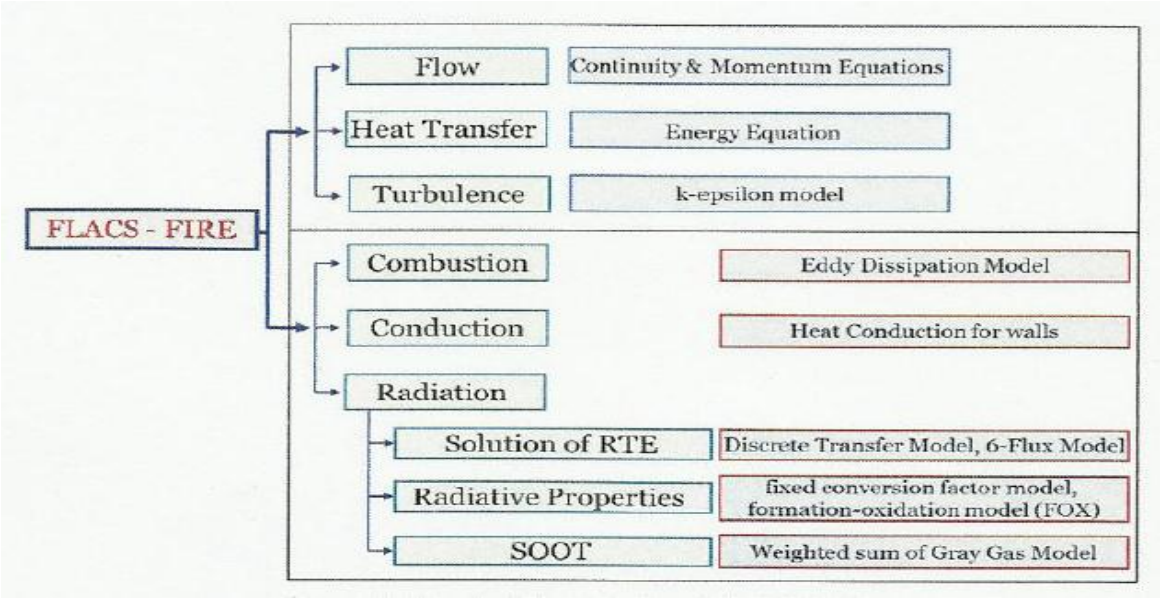

Figure 3-2 *Key building blocks of FLACS-Fire [15]*

3.3 Mathematical description of turbulent reacting flows

To solve the flow physics, CFD divides the domain of interest into a number of smaller, non-overlapping subdomains. This results in the generation of a mesh (or grid) of cells (control volumes) covering the whole domain of interest. The fluid flows in each of these cells are usually solved numerically through fundamental equations governing the fluid dynamics. These equations are based on conservation laws of physics: the conservation of mass (continuity), Newton`s second low for the conservation of momentum, and the first law of thermodynamics for the conservation of energy. All the fluid governing equations can be expressed by a one general transport equation for any variable property Φ [13]

$$\frac{\partial}{\partial t}(\rho\Phi_i) + \frac{\partial}{\partial x_j}(\rho\Phi_i u_j) = \frac{\partial}{\partial x_j}\left(\Gamma_i \frac{\partial\Phi_i}{\partial x_j}\right) + S_i \qquad \textbf{Eq. (3.1)}$$

1 2 3 4

Where Φ_i represents a scalar variable, for example velocity (u_i), enthalpy (h), mass fractions of species (Y_i) or mixture fraction (ξ), while 1 is the transient term, 2 is the convective term, 3 is the diffusive term and 4 is the source term. This property ϕ is function of three space coordinates and time. Thus,

$$\Phi = \Phi(x, y, z, t) \qquad \textbf{Eq. (3.2)}$$

Where x, y, z, and t are the independent variables. Dependence on three space coordinates leads to a three-dimensional geometry. Time dependence situation is called unsteady. Otherwise, it is called steady.

The governing equations include such unknown quantities as turbulence stresses (or Reynolds stresses), turbulent fluxes and source terms. Turbulence fluxes can be described by turbulence modeling. Unknown source terms (the net production rate of species in conservation equation of mass fraction of species and the net rate of heat generation by radiation in conservation equation of energy) can be found by fire modeling.

3.4 Turbulence theory and turbulence modeling

Most practical fires are turbulent in nature. The motion of turbulent flow is unstable and unsteady with a broad range of vortices (eddies) generated by shear stress within flow due fluctuations in velocity which can lead to fluctuations in scalars such as density, temperature, and mixture composition. The turbulent flows include a wide range of turbulent scales. The large turbulent scales can be described by characteristic turbulent length (l'), velocity (u') and time scale (τ'). These structures are responsible for transport of turbulent kinetic energy. The small turbulent scales described by Kolmogorov scales of velocity (u^*), length (l^*) and time (τ^*). More detailed about these scales are described in combustion modeling (See Section 3.5)

There are three methods for solving turbulent equations: Reynolds averaged Navier-Stokes, RANS or Favre-Averaged Navier-Stokes, FANS, Large-Eddy Simulation, LES and Direct Numerical Simulation DNS [9].

In RANS-based turbulent models, the turbulent flows described by Reynolds-averaged conservation equations (RANS) for constant density flows, and known as RANS or Favre-averaged equations for non-constant density flows. In reacting flows a large changes in density occur due to the heat release of the reaction and additional terms appear due to the correlation of scalar and density fluctuations. By Favre-averaging the general property ϕ is defined as

$$\tilde{\phi} = \frac{\overline{\rho\phi}}{\bar{\rho}} \qquad \textbf{Eq. (3.3)}$$

where $\bar{\rho}$ is density and the overbar indicated Reynolds-averaged quantity. An instantaneous value of general property (mass, velocity, enthalpy, chemical species) is decomposed into the Favre-averaged and its fluctuation value by $\phi = \tilde{\phi} + \phi^{"}$. The Favre-averaging reduces the number of unknown quantities (only the Reynolds stress and turbulent flux terms) and very practical in many numerically related fire investigations. By turbulence modeling can man find and describe these unknown quantities in terms of known. Turbulence is generally very complex and varied. No single turbulence model can be found to span all turbulence states because none is to be valid for all types of flows.

Boussinesq (1877) first introduces the eddy or turbulent viscosity concept by suggesting that Reynolds stresses are linked to the mean rate of eddy deformation (strain). The turbulent stresses can be modeled by employing Favre -averaging [16]

$$-\bar{\rho}\,\widetilde{u_i^{"}u_j^{"}} = \mu_t\left(\frac{\partial\tilde{u}_i}{\partial x_j} + \frac{\partial\tilde{u}_j}{\partial x_i}\right) - \frac{2}{3}\left(\bar{\rho}\tilde{k} + \mu_t\frac{\partial\tilde{u}_i}{\partial x_j}\right)\delta_{ij} \qquad \textbf{Eq. (3.4)}$$

where μ_t is the turbulent or eddy viscosity and $\tilde{k}$ is the turbulence kinetic energy. This approach describes the unknown Reynolds stresses with an unknown turbulent viscosity.

The dynamic turbulent viscosity can be obtained from dimensional analysis [16]

$$\mu_t = \bar{\rho}\,v_t = \bar{\rho}\sqrt{k}l^{'} = C_\mu\bar{\rho}\,\frac{\widetilde{k^2}}{\tilde{\varepsilon}} \qquad \textbf{Eq. (3.5)}$$

where ν_t is kinematic viscosity $\nu_t = u^{'} \times l^{'}$, $u^{'}$ is characteristic velocity and defined as $k^{1/2}$, and $l^{'}$ is the characteristic length defined as $\frac{k^{3/2}}{\varepsilon}$, $C_\mu$is an empirical constant. The values of k and ε can be found through solution of their respective transport equations.

The standard $\kappa - \varepsilon$ model by Launder and Spalding (1974) [17] has become widely used model for industrial applications of turbulent flows. This model is based on eddy viscosity concept and included two transport equations: transport equation for turbulent kinetic energy, k and transport equations for the dissipation rate of turbulent kinetic energy, ε. Transport equations for the standard $\kappa - \varepsilon$ model defined as

$$\frac{\partial}{\partial t}(\bar{\rho}\tilde{k}) + \frac{\partial}{\partial x_j}(\bar{\rho}\tilde{k}\tilde{u_j}) = \frac{\partial}{\partial x_j}\left[\left(\mu + \frac{\mu_t}{\sigma_k}\right)\frac{\partial \tilde{k}}{\partial x_j}\right] - \bar{\rho}P_k - \bar{\rho}\tilde{\varepsilon} \qquad \textbf{Eq. (3.6)}$$

$$\frac{\partial}{\partial t}(\bar{\rho}\tilde{\varepsilon}) + \frac{\partial}{\partial x_j}(\bar{\rho}\tilde{\varepsilon}\tilde{u_j}) = \frac{\partial}{\partial x_j}\left[\left(\mu + \frac{\mu_t}{\sigma_\varepsilon}\right)\frac{\partial \tilde{\varepsilon}}{\partial x_j}\right] - C_{1\varepsilon}\frac{\tilde{\varepsilon}}{\tilde{k}}\bar{\rho}P_k - C_{\varepsilon 2}\bar{\rho}\frac{\tilde{\varepsilon}^2}{\tilde{k}} \qquad \textbf{Eq. (3.7)}$$

The constants for the standard $\kappa - \varepsilon$ model suggested by Launder and Spalding [17]:

$C_\mu = 0.09, \sigma_k = 1.0, \sigma_\varepsilon = 1.3, C_{\varepsilon 1} = 1.44, C_{\varepsilon 2} = 1.92$

Finding k and ε are input to the model expression for the eddy viscosity in Eq. (3.5), and hence, the turbulence stresses in Eq. (3.4) can be found. The standard $\kappa - \varepsilon$ model model is easy to implement and it is a practical in use and it is more numerically stable, but it is incapable to reproduce the stabilizing/destabilizing influences of swirling motions and buoyancy forces, the effects of strong streamline curvature, and variable density pressure gradient influences.

3.5 Combustion and combustion models

Combustion of practical fires is full of complex exothermic chemical reactions and greatly influenced by turbulence. Understanding the chemical kinetics in fires is a branch of chemical science that studies the rates of chemical reactions. All chemical reactions take place at a definite reaction rate. The reaction rate defines as the rate of formation or consumption of a species in a chemical reaction [9]. They are strongly influenced by number of important systems conditions such as concentrations of the chemical compounds, surrounding pressure, temperature, presence of a catalyst or inhibitor, and the effects of radiation heat transfer.

Combustion processes are never perfect or complete in reality. The chemical reaction in the fires involves a series of elementary steps in which highly reactive intermediates (atoms and free radicals) are formed. The complexity increases with the size a structure of the fuel molecule.

In field modeling, simplified reaction mechanisms consisting of one or several global reaction are used to describe chemistry. Numerical models of large-scale flames with a large number of species in two- or three-dimensional geometries may not be able to use detailed reaction mechanism due to the enormous computational costs. Computer time is roughly proportional to number of species. In a state of complete combustion, the reaction mechanism can be simplified and expressed in a one single step elementary reaction:

$$Fuel + Oxydant \xrightarrow{k_f} Product \qquad \textbf{Eq. (3.8)}$$

The rate of reaction is proportional to the collision of the fuel and oxidant molecules. At a given temperature, the number of collisions is proportional to the products of the concentrations of reactants in the mixture. The reaction rate of the fuel can be expressed as

$$R_f = -k_f \bar{\rho}^2 C_f C_{ox} \qquad \textbf{Eq. (3.9)}$$

Where $C_f$and $C_{ox}$are concentrations to fuel and oxidant, k_f is the proportionality constant called the specific reaction rate constant. This value depends on temperature. This temperature dependence can be described by Arrhenius low [7]

$$k_f = A_0 \exp\left(-\frac{E_a}{RT}\right) \qquad \textbf{Eq. (3.10)}$$

where $E_a$is the activation energy (J/mol), R is the universal gas constant (8,314 J/Kmol) and T is the temperature (K). The constant A_0 is known as the preexponential factor (collision factor).

The expression for time averaged reaction rate based on Reynolds decomposition and ideal-gas low [13] can be written as

$$\bar{R}_f = \frac{Ap^2}{R} \bar{T}^{n-2} exp\left(-\frac{E_a}{R\bar{T}}\right) \bar{Y}_f \bar{Y}_{ox} (1 + F) \qquad \textbf{Eq. (3.11)}$$

Where $\bar{Y}_f$ and $\bar{Y}_{ox}$ are mass fractions of the fuel and oxygen, the term F includes the influence of turbulence. The complexity of the time averaged reaction rate occurs due to the many correlation terms. The use of the Eq. (3.12) is limited. Therefore, the various combustion models are used in combustion modeling for to overcome non-linear terms.

For combustion, the governed process determines the appropriate selection of suitable models. Most practical fires occur at high flame speed where eddy mixing governs the combustion process between the fuel and the oxidizer. For turbulent flames assumption of fast chemistry simplifies the problems of the chemistry-turbulence interactions, since molecular species of concentrations are related to scale. In combustion modeling, the interactions between turbulence and chemistry play important role and must be modeled. One useful dimensionless parameter to characterize combustion process is Damköhler number, Da which can be expressed as

$$Da = \frac{\tau}{\tau_c} = \frac{time\ scale\ of\ turbulent\ mixing}{time\ scale\ of\ combustion\ chemistry} \qquad \textbf{Eq. (3.12)}$$

when τ is larger than τ_c, Da>1, the mixing of reactants is slow and the reaction process is controlled by eddy mixing (diffusion process).The slowest process is governed reaction process. The reactants are reached the suitable temperature and concentration and reacts as soon as they mixed. However, when τ is small, Da<1, this corresponds to a large dissipation rate of eddies and rapid mixing. The reaction is governed by chemistry. Reactants are mixed, but they will react at appropriate temperature and concentration.

The flame behavior can be described by Borghi diagram in Figure 3-3.

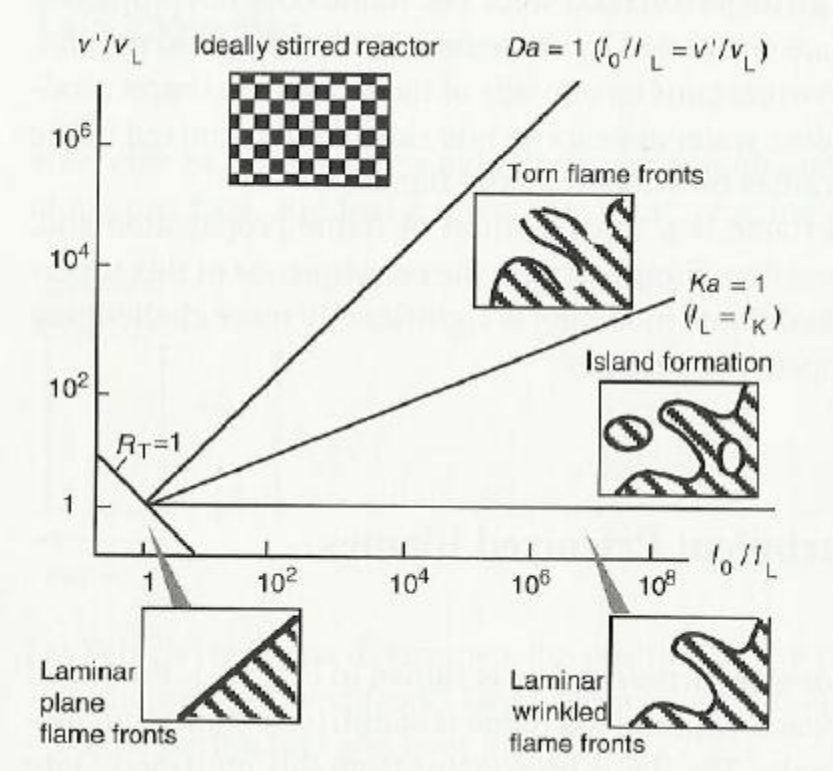

Figure 3-3 *Borghi diagram [9]*

The diagram divided into several domains with different flame behavior. Laminar combustion is observed when the turbulent Reynolds number is smaller than 1. When the Reynolds number is over 1, the domain with turbulent combustion divided into three zones: flamelet regime (is below the *Ka=1*), well-mixed reactor or perfectly stirred reactor regime (is above *Da=1*), distributed reaction zone is between two other regimes) [9]. The high turbulent flames are characterized with high turbulent velocity scale and very small turbulent length scale. The flame has broad reaction zone and all turbulent eddies are embedded in the reaction zone. On the Borghi diagram, this regime is in the domain of ideal stirred reactor. The Damköhler number is lower than 1 in this domain. It means that the chemical time scale is larger than the turbulent mixing time scale.

Combustion models are used for to solve the source term in conservation equation for a single species *i* expressed by its mass fraction, Y_i.The source term represents the net production rate of species *i* due to chemical reaction.

Combustion models

The Eddy break-up model [18] was developed by Spalding , which allows that reaction rate is based on the species concentration fluctuations and the rate of break-up of eddies. This model requires the solution to the mass fractions of the fuel, oxidant and products and additional correlations. The Eddy Dissipation model (EDM) was presented by Magnussen and Hjertager [19] where the reaction rate is governed by the mean species concentrations, not fluctuations of the species concentration. The Eddy Dissipation and the Eddy break-up models are alternative approaches to treat turbulent non-premixed flames and premixed flames. Reaction rates of both models are related to the time required to mix reactants. The mixing time is dominated by the eddy properties and therefore the rate is proportional to the mixing time defined by the turbulent kinetic energy and dissipation.

In the present work, the Eddy Dissipation Concept (EDC) was used to model interactions between chemistry and turbulence. This model was developed by Magnussen and Hjertager [19] and has later been extended by Magnussen[20].

Eddy Dissipation Concept

EDC is based on turbulent energy cascade where the turbulent kinetic energy is transferred stepwise from the mean flow to large eddies and then further to smaller and smaller eddies as shown in Figure 3-4.

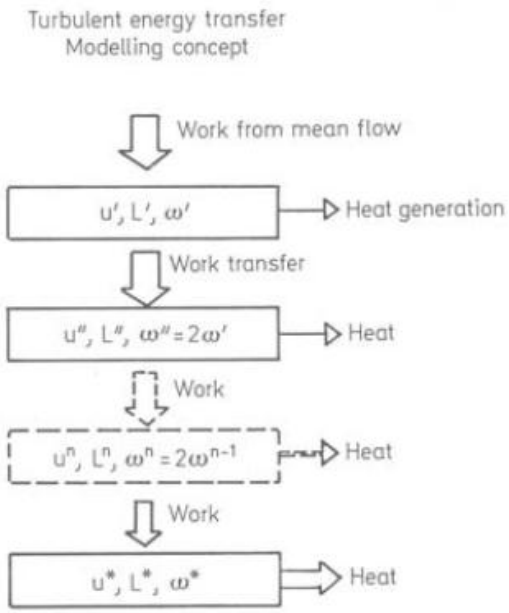

Figure 3-4 *Concept of transfer of energy from bigger to smaller structures [21]*

The larger eddies carry the major part of the kinetic energy. They represent the first level in the energy cascade. The larger scales are calculated by turbulent modeling, in terms of turbulent kinetic energy, k and its dissipation, ε.

The length scale of larger eddies, $l^{'}$ and time scale, $\tau^{'}$ can be written as

$$l^{'} = \frac{k^{3/2}}{\varepsilon} \qquad \textbf{Eq. (3.13)}$$

$$\tau^{'} = \frac{k}{\varepsilon} \qquad \textbf{Eq. (3.14)}$$

The smaller scales, Kolmogorov scales of length, l^{*} and time, τ^{*} and velocity, u^{*} can be expressed as function of larger scales through the turbulent energy cascade [21].

The smallest eddies contain less energy but they have the highest frequency and the largest viscous stresses. The dissipation of energy occurs at all scale levels by viscous forces but is largest in the smaller eddies.

EDC model is based on the assumption that the chemical reaction occurs in the fine structures where the dissipation of turbulent energy is largest. It is assumed that the fine structures can be treated as homogeneous, constant pressure reactors. (See Figure 3-5)

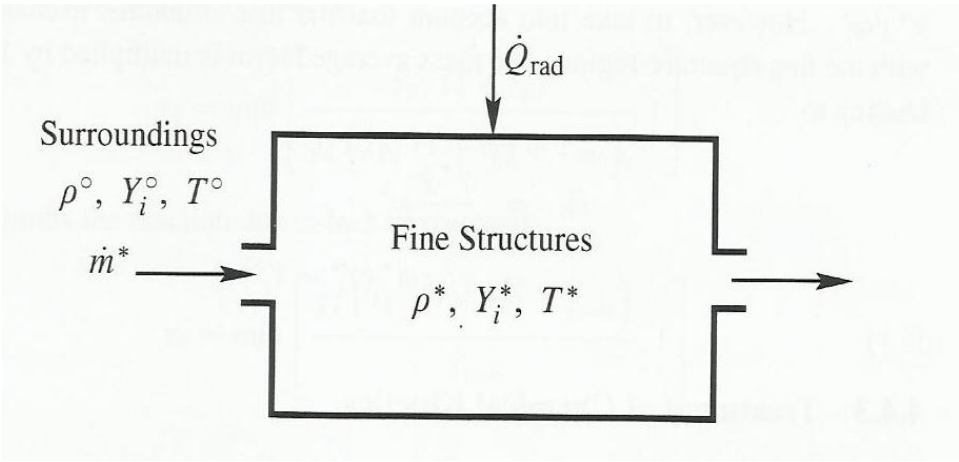

Figure 3-5 *Schematic homogeneous reactor of fine structure [22]*

Assuming that chemical reactions take place in the fine structures, the reaction rate of species, i per time and volume of all fluid (reactor +surrounding fluid) calculated from a mass balance of the fine structure reactor and the net mean reaction rate of species, i is expressed as

$$-\bar{R}_i = \bar{\rho}\dot{m}\chi\left(Y_i^\circ - Y_i^*\right) \qquad \textbf{Eq. 3.15}$$

where Y_i^* and Y_i^o represent the mass fractions of species, in reacting (fine structures) and non-reacting (surrounding fluid) part, respectively. χ is the reacting fraction of the fine structures and is modeled as

$$\chi = \chi_1 \cdot \chi_2 \cdot \chi_3 \qquad \textbf{Eq. (3.16)}$$

where χ_1 is the probability of coexistence of the reactants, χ_2 is the degree of heating and χ_3 limits reaction due to lack of reactants.

$\dot{m}$ can be expressed as

$$\dot{m} = \dot{m}^*\gamma^* \qquad \textbf{Eq. (3.17)}$$

Where $\dot{m}^*$ is the mass exchange rate between fine structures and surrounding fluid divided by the mass of fine structures.

$$\dot{m}^* = 2\frac{u^*}{L^*} = 2.5\left(\frac{\varepsilon}{\nu}\right)^{1/2} \qquad \textbf{Eq. (3.18)}$$

γ^* is the mass fraction of fine structures in the flow .

$$\gamma^* = \left(\frac{u^*}{u'}\right) = 9.8\left(\frac{\nu\varepsilon}{k^2}\right)^{3/4} \quad \textbf{Eq. (3.19)}$$

In simulations, the mean values of mass fraction are required. The mean mass fraction can be obtained from the linear combination of properties in the fine structures and the surrounding fluid as follow equation

$$\tilde{Y}_i = \gamma^*\chi Y_i^* + (1-\gamma^*\chi)Y_i^\circ \quad \textbf{Eq. (3.20)}$$

Then the mean chemical reaction rate can be written as

$$-\bar{R}_i = \frac{\bar{\rho}\dot{m}\chi}{(1-\gamma^*\chi)}(\tilde{Y}_i - Y_i^*) \quad \textbf{Eq. (3.21)}$$

The simplest and most widely used expression is assuming infinitely fast chemistry where chemical reactions occur “infinity fast”. Then the mean chemical reaction rate can be written as

$$-\bar{R}_f = \frac{\bar{\rho}\dot{m}\chi}{(1-\gamma^*\chi)}\tilde{Y}_{min} \quad \textbf{Eq. (3.22)}$$

where

$$\tilde{Y}_{min} = \min(\tilde{Y}_{f,}\frac{1}{r}\tilde{Y}_{ox}) \quad \textbf{Eq. (3.23)}$$

3.6 Radiation models

Thermal radiation plays an important role in overall heat transfer in fire simulations. Energy is transferred from high temperature gas to surroundings of colder temperature by radiation. This transfer of heat will lead to lower combustion temperature. This energy loss is represented by source term in the transport equation for enthalpy. The gas temperature and composition of the burning gas will influence on amount of this heat transfer. An accurate modeling of the radiation is required for a good fire model. Radiation calculations are more difficult to incorporate into the models. Two radiation models have been developed in FLACS; the six-flux model and the Discrete Transfer Model [23]. In the present work, the Discrete Transfer Model was used in calculations of radiation.

Discrete Transfer Model

The Discrete Transfer Model (DTM) assumes that the intensity through solid angle is approximated by a single ray, because the rays are fire from surface elements into a finite number of solid angles that cover hemisphere about each element [15]. The number of rays and directions are decided before. The DTM solves the radiative transfer equation (RTE) for each ray from solid boundary to another solid boundary in geometry. The RTE describes the radiation intensity field in an absorbing, emitting and scattering medium. This method can calculate intensity distribution in arbitrary shaped, three dimensional complex geometries. Rays are fired from solid boundaries and traces through the volume. The distance travelled in

each control volume is used for calculating of radiation source term. At the boundary the boundary conditions of radiative heat transfer are used to determine the intensity of rays fired from that surface. The input parameters that characterize the wall and the medium (gas temperature and absorption coefficient of the medium, temperature and emissivity of walls, number of rays and directions) are needed for the radiative transfer calculations. The absorption coefficient is calculated using Mixed Gary Gas Model of Truelove [24] that solves transient temperature and mole fractions of CO_2, H_2O and soot.

3.7 Soot models

Correct prediction of soot is important for the calculation of radiation. Soot particles will absorb and emit energy from the flame. The thermal radiation from soot will influence on peak temperature in the flame. The mechanisms for soot formation, growth and oxidation are difficult phenomena in the combustion process. These phenomena are influenced by the flame temperature. Two models for soot handling are implemented in FLACS-Fire. A fixed conversion factor model (CFM) and a formation-oxidation model (FOX) [15].

In FLACS-Fire the soot formation has been modeled by the Magnussen soot model [19] where the soot is formed from gaseous fuel in two stages: formation of radical nuclei and soot particle formation from these radical nuclei. Intermediate species are not included in FLACS-Fire due to limitations of memory and the computational time. There are two possibilities for handling of soot in FLACS-Fire:

1. **A fixed conversion factor model**

A certain amount of carbon in fuel is converted to soot in the products directly. The amount of carbon transformed to soot depends only on the fuel composition and is independent of the equivalence ratio, temperature, time, etc. This is a crude model.

2. **Formation-oxidation model (FOX).**

This model has two source terms in the transport equation: a formation of soot and the oxidation of soot. It is possible to run simulation without any soot model.

The soot consists mostly of carbon and small amount of hydrogen. The size and structure of soot varies. The soot formation process in flames can be divided into 5 steps: soot inception, soot surface growth, oxidation, coagulation and agglomeration [9]. The soot models assumed that the soot particles are formed from large polycyclic aromatic hydrocarbons (PAH). The acetylene (C_2H_2) is supposed to be key molecule in formation of the first aromatic ring. The growth of the ring formed molecules by addition of acetylene leads to the soot surface growth. The small soot particles will coalesce into larger particle when they collide and stick to each other. The soot particles will also be oxidized by O atoms, OH radicals and O_2. The larger soot particles will form chain and grow into larger soot aggregates. The surface growth of larger particles is slower than the smaller particles.

3.8 Wall heating (conductive heat transfer)

Heating of solid walls is necessary to include in fire modeling. Materials change properties due high temperatures and they extend their size, which may have dramatic consequences for

the construction. Heat conduction into the wall leads to loss of a large portion of the total heat transfer; this can influence the accuracy of the indoor gas temperature. The wall temperature is an important output from fire simulation.

4 Literature review

A large number of pool and jet flames have been studied in a detailed by both experimentally and numerically the last four decades. Experimental data obtained from those studies are significant for understanding the physics and behavior of fully-developed fires. Results from experiments are important for performing validation of simulations and development of software. In this chapter, the experimentally and numerical survey of vertical jet fires and pool fires is presented. The object of this search was to find the available experimentally data that could be relevant in validation process of the fire model through FLACS-Fire simulations.

4.1 Study of vertical jet fires

A. Coppalle and D.Joyeux [25] studied experimentally turbulent non-premixed jet flame of ethylene in still air. The mean and fluctuating values of temperature and soot fractions were measured across the jet. They studied three flames with the different Reynolds numbers (momentum driven, slightly influenced by the buoyancy effects and buoyancy driven). The maximum concentration of soot in the flame that is momentum driven was greater than in the flame that is completely driven by the buoyancy effects. The turbulence transport is efficient in the momentum driven flame.

Lionel Tessé et al. [26] studied numerically the influence of the turbulence-radiation interaction in a turbulent non-premixed ethylene jet flame of A. Copalle and D.joyeux. Radiation transfer within sooty turbulent flame of ethylene was calculated by using a Monte Carlo method and an CK model for the gases. Turbulence was modeled by $\kappa - \varepsilon$ model. Turbulence-radiation interaction increased the radiative heat loss. Soot particles played the most important role in calculation of the radiative heat transfer. The peak of soot concentration was located in very narrow zone at the center of flame that corresponds to the fuel side.

Rune Natten Kleiveland [22] studied the jet flame of ethylene by use of the SPEIDER code. The focus of his work was to study the ability of the EDC to handle soot models. The soot models includes two-way coupling of soot and gas-phase chemistry. The predictions were performed with the fast chemistry assumption. The effect of radiation on soot formation and temperature was studied. The results of soot volume fractions were overestimated compared to experimental measurements. The predicted temperatures at different axial and radial locations were generally in good agreement with measured values.

Experiments of propane jet flame in still air were performed by A. Palacios et el. [27]. The flames up to 10 m were obtained using different exit diameters (10mm-43.1mm). The experiments were filmed with video and thermographic camera. The visible and infrared images were used to determine the flame height and lift-off distance. Jet heights were expressed as function of mass flow rate, exit diameter, Froude number and Reynolds number. The results showed that the flame height is increased with the orifice diameter and the fuel mass flow rate.

An axial temperature distribution in vertical jet fire of propane was studied experimentally by Mercedes Gomez-Mares at al. [28]. The temperature along the jet fire centerline was

measured using a set of thermocouples and the flame contours were determined from infrared images. The results of temperature along the jet fire centerline showed that temperature increased from the bottom of the flame, reached a maximum value and decreased again at the top zone. The temperature measurements inside the flame were around 1600 K at 90% of the flame length. Therefore, it was decided to use the temperature of 1500 K for comparing the data of lengths.

Christopher Nilsen [29] evaluated the FLACS-Fire version 2.2.7 on jet diffusion flame. The radiation model used in his simulations was the six-flux radiation model. The numerical predictions gave good results on flame heights and flame temperatures in the centerline of vertical flames with low mass flow velocity. Results of larger jet flames showed that the flame heights were increasingly over predicted when the mass flow rate increases. Radiation intensity was too high and incorrectly distributed.

4.2 Study of pool fires

Chin-Hung Lin et al. [30] investigated numerically the radiative flux, the flame shape and the flame height of heptane pool fire with diameter 0.3m. Turbulence was modeled by LES model and combustion was modeled by the mixture fraction combustion model. Radiation was handled using the radiative transport equation for a non-scattering gas model a narrow-band model. The used grid was uniform over the simulated domain ($1.5\times1.2\times2.5(m^3)$). As well known, the simulation accuracy depends strongly on the resolution of the mesh. The predicted flame length with fine grid resolution was similar to the flame length calculated by Heskestad correlation. The difference between the predicted flame temperature and that obtained experimentally was from 60 to 135℃.

Lars Roar Skarsbø [31] studied the pool fire of heptane through experimental work and CFD simulation using FLACS and FDS. Heptane fuel was located in a pan with square sides of 0.5m. Maximum temperature measured at the center line was in region 700-800 ^{0}C. FDS simulations showed that the predictions of the temperature, velocity, evaporation rate were grid dependent. Small grid cells were required to get numerical results close to experimental results. Simulation with FDS showed a good prediction of results. Simulations using FLACS-Fire showed that the results of temperature at the centerline were over predicted comparing with experimental results. Under plume layer and around the fire, the temperature deviated more from experimental values. Simulating the fire with horizontal jet nozzles or combination of horizontal and vertical jet nozzles resulted in flame temperatures closer to experimental results.

The overview of experiments from the literature search used in the present work is presented in the Table 4-1.

Table 4-1 *The review of relevant experiments collected from literature search*

Description	Diameter	Velocity / mass flow rate	Measurements	Code	References
Vertical jet fire of ethylene	D=4mm	29.5m/s	Temperature	FLACS	[25], [26]
	D=3mm	52.0m/s	Temperature at different flame locations, soot volume fractions and mixture fraction	SPIDER FLACS	[22], [32]
Vertical jet fire of propane	D=12.75mm	150m/s or 0.034kg/s	Flame length, Temperature at the centerline	FLACS	[33],[27]
	D=20mm	250m/s or 0.125kg/s			
Pool fire of heptane	D=0.3m	0.00145kg/s	Centerline temperature of flame	FDS and FLACS	[30]
	D=0.5m	0.0464kg/s			[31]

5 Simulations with FLACS-Fire

This chapter presents the modeling of turbulent non-premixed flames described in the Table 4-1 using FLACS-Fire. The experiments used for comparison with simulations were chosen on background of the detailed descriptions of the experimental set-up and measured data for validation of the FLACS-Fire model.

5.1 Fire modeling in FLACS

For all simulations of fire, the governing equations of fluid flow for mass, momentum, enthalpy and mass fraction of species were solved in FLACS on 3-D Cartesian grid using a finite volume method. The numerical handling of turbulent flows was simplified by the introduction of mean quantities (Favre-averaged equations). However, it causes unknown source terms in the Favre-averaged transport equations. Solving them requires additional models: combustion model, radiation model, soot model and turbulence model.

Combustion was modeled by the Eddy Dissipation Concept model with assumption of fast chemistry, where the chemical reaction is one-step, irreversible and infinitely fast. The turbulence flow field was modeled by the standard $k-\varepsilon$ model. The radiation was modeled using the Discrete Transfer Radiation Model and soot was handled with the Magnussen soot model [19].

The diameter and fuel velocity of simulated propane jets, ethylene jets and heptane pool fires are given in Table 4-1.

The setup file was used for to specify the combustion model, the radiation model and the soot model. The used setup in the present work is presented below:

```
VERSION 1.1
 $SETUP
  COMBUSTION_MODEL=”FIRE”
  KEYS=”RADIATE=01, SOOT_MODEL=2”
  KEYS=”RADMODD=100”
$END
```

The simulations of pool flames and propane jet flames were simulated without soot model. The simulated results were obtained from steady state solution. The measured values were defined as monitor points. In all simulations, the flame was assumed ideally axisymmetric.

In simulations of ethylene jet fire, the different grid cell size has been used. In addition, the changes in such parameters as Courant-Friedrich-Levy number based on speed on sound (CFLC), the relative turbulence intensity (RTI), the turbulent length scale (TLS) and the number of rays were tested. The influence of radiation modeling on temperature was tested in simulations without radiation model.

The simulations of pool fires are based on the fuel evaporation model where evaporation of liquid fuel was modeled by many jet nozzles (leaks). The total fuel flow rate and surface area of pool were divided by number of leak.

Operating conditions in simulations of jet and pool fires are shown in Table 5-1.

Table 5-1 *Operating conditions for jet and pool fires*

Conditions	**Ethylene jet fire of D=4mm**	**Ethylene jet fire of D=3mm**	**Propane jet fire**	**Heptane pool fire D=0.3m**	**Heptane pool fire D=0.5m**
Absolute pressure (atm)	1	1	1	1	1
Fuel temperature (K)	323	323	298	293	293
Air temperature (K)	293	293	303	293	293
Turbulence Intensity	0.05	0.06	0.1	0.01	0.1
Turbulent Length Scale (m)	0.004 (equal nozzle diameter)	0.003 (equal nozzle diameter)	0.01275 (equal nozzle diameter)	0.015 (20% of nozzle diameter)	0.02 (20% of nozzle diameter)
CFLC	100 for basic case	100	37.5 for jet of 150m 50 for jet of 250m/s	20	20
CFLV	2	2	0.5	0.5	0.5

CFLC and CFLV values (Courant-Friedrich-Levy numbers) connect simulation time step length to control volume dimension through signal propagation velocity (CFLC number based on sound velocity, CFLV based on fluid flow velocity) [14].

6 Results and discussion

In this chapter, the numerical predictions of temperature, flame length, soot mass fractions, mixture fraction for turbulent diffusion flames were presented graphically and compared with experimental data and simulation results of other authors. The comparison between predicted and experimental results was validated and discussed.

6.1 Vertical jet flame of ethylene with D=4mm

The objective in modeling of ethylene jet flame was to perform the grid sensitivity analysis and test the prediction results of temperature with changed parameters in FLACS. The temperature profiles of ethylene jet flame under different conditions were compared with experimental temperature measurements [25] and results predicted by Tessé et al. [26].

6.1.1 Grid sensitivity analysis

To make sure the solution is not dependent of the grid, simulations have been performed with three different grid cell sizes: 6mm, 4mm and 2mm. The finest grid within the flame boundary was uniform in x- and y- directions. The grid size in z-direction was 0.02m and 0.01m. Outside the boundary, the grid was stretched in all directions.

The simulation with grid size of 2mm was presented with four nozzle jets, where area of each was equal $3.14\times10^{-6}m^2$.

Radial profiles of predicted temperature in the middle of flame with three different grid cell sizes are shown in Figure 6-1. On the left side, the grid cell size in z-direction is 0.02m, while one the right side the grid cell size in z-direction is 0.01m.

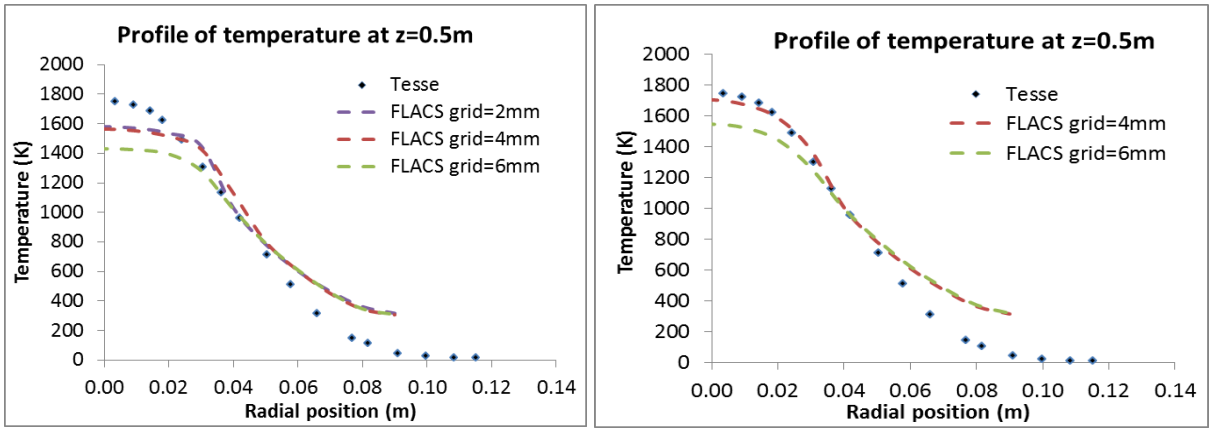

(a) Grid cell size in z-direction is 0.02m (b) Grid cell size in z-direction is 0.01m

Figure 6-1 *Radial profiles of the temperature with different grid resolutions at axial position 0.05m*

Results from the simulations of Lionel Tessé [26] are presented with symbol. The dashed lines show temperature results with different grid cell size from the simulations by FLACS-

Fire. The simulations with size of grid cell 2mm and 4mm are in much closer agreement with the Tessé results than the simulation with cell size of 6mm.

The best temperature results were predicted with grid cell size of 0.004m×0.004m×0.01m where total number of used cells was 69 803. (See in Figure 6-1 (b)-red dashed line) The total used number of cells with largest grid cell size 0.006×0.006×0.02 was 16 928. The temperature results of this mesh had largest difference from results reported by Tessé (See in Figure 6-1 (a)-green dashed line). Radial profiles of temperatures at location between 0.03m and 0.05m for all grids size are generally in good agreement with Tessé values. Close to the centerline the temperatures are under predicted in all simulations. At the outer part of the flame, the predicted temperatures decreased too rapidly and over predicted. Simulations with largest mesh resolution improved significant the temperature results near centerline of flame (See Figure 6-1 (b)). Simulation with size of grid cell 0.002m×0.002m×0.01m is crashed. Therefore, the results of this simulation are not presented here.

Profile of predicted temperature at the centerline of flame with different grid resolution and experimental values are shown in Figure 6-2. The influence of radiation model on predicted results of temperature is presented in Figure 6-2 (b) where the simulations were performed with radiation model.

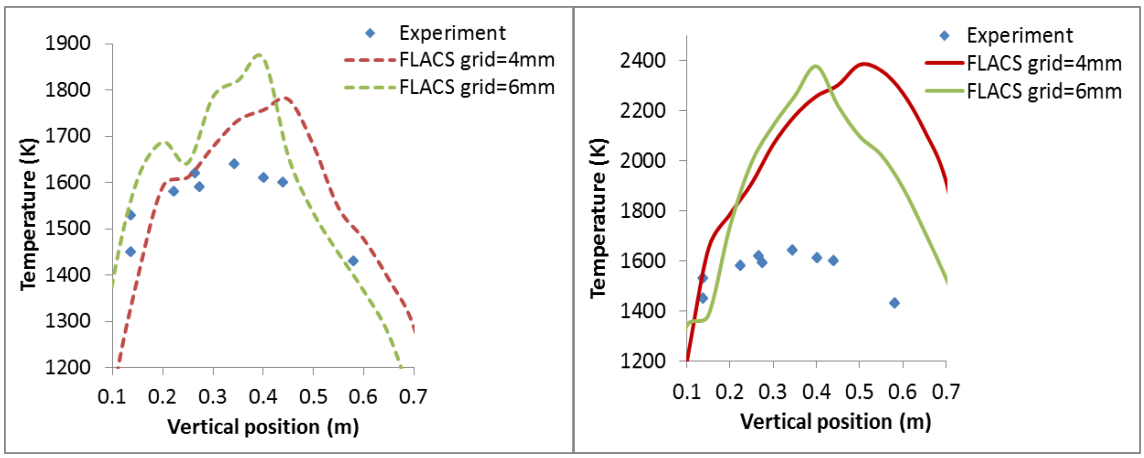

(a) With radiation model (b) Without radiation model

Figure 6-2 *Predicted temperature at centerline of flame with radiation model (a) and without radiation model (b)*

The predicted results of temperature with radiation model are much closer to experimental measurements than the temperature results without radiation model. The peak of temperature without radiation model is 2384K for simulation with grid cell size 4mm and 2378K for grid size of 6mm (see Figure 6-2 (b)). In simulations with radiation model, the predicted peak of temperature was respectively 1780K and 1869K (see Figure 6-2(a)). The peak of temperature in simulations without radiation model is around 510-610K higher comparing with temperature results where radiation model is included. The difference in the peak of temperature between numerical results with radiation model and experimental measurements is around 140-229K. The predicted results of temperature with radiation model and smallest grid cell size are closer to the experimental values than simulation with grid cell size 6mm.

6.1.2 Parametric sensitivity analysis

The calculations with the grid cell size 0.004m×0.004m×0.01m were found to produce grid independent results. Therefore, the base case of this grid size with grid size was chosen to use further in the parametric studies.

Changes in such parameters as Courant-Friedrich-Levy numbers based on speed of sound, (CFLC), Relative Turbulence Intensity (RTI), Turbulence Length Scale (TLS) and number of rays (RADMODD) were tested in simulations of the base case.

Detailed description of the base case and its tested parameters are shown in the Table 6-1.

Table 6-1 *Description of the base case and tested values*

Parameter	**Base case value**	**Tested values**
CFLC (simulation time step based on speed of sound)	100	20, 60, 150
RADMODD (number of rays)	100	10 and 200
RTI (Relative Turbulence Intensity)	0.05 (medium)	0.1(high) , 0.01 (low)
TLS (Turbulent Length Scale)	0.004 (equal nozzle diameter)	0.0004 (10% of nozzle diameter) and 0.002 (50%)

The radial temperature profiles with changed CFLC number, RTI, TLS and RADMODD number are shown in Figure 6-3.

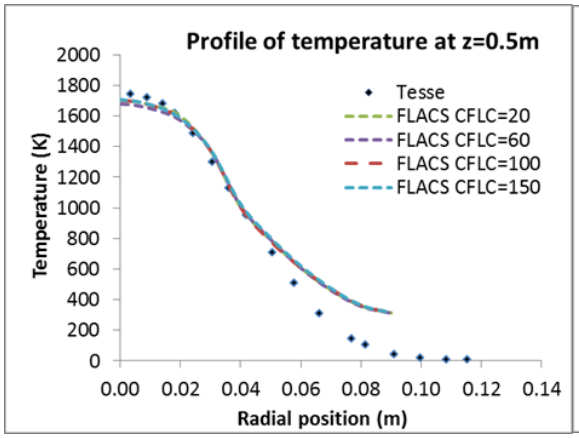

(a) Temperature with changed CFLC

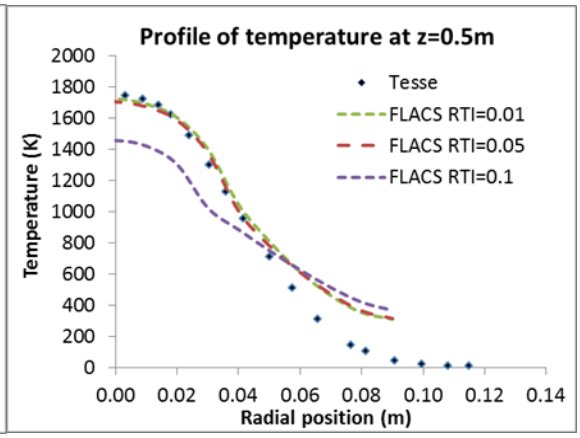

(b) Temperature with changed RTI

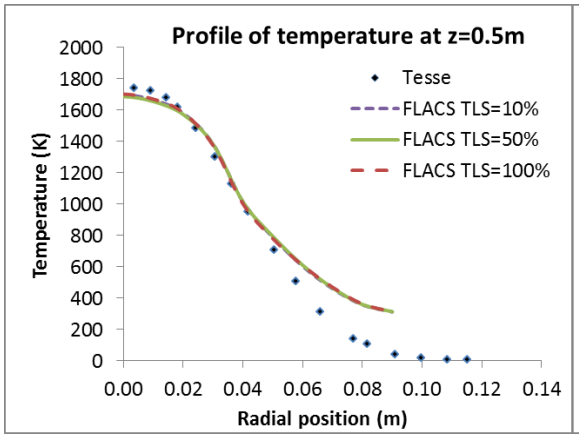

c) Temperature with changed TLS

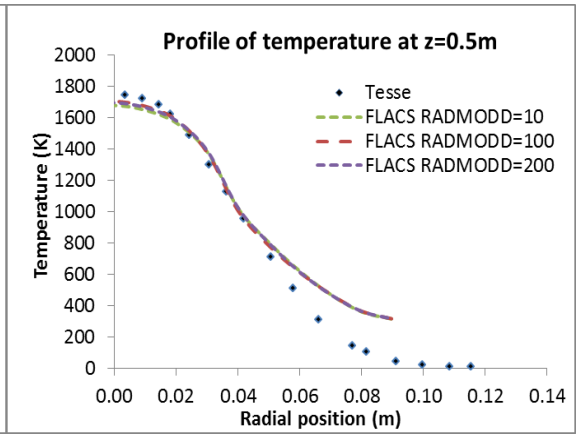

d) Temperature with changed RADMODD

Figure 6-3 *Radial temperature profiles at axial location 0.5m with changed parameters; CFLC, RTI, TLS and RADMODD*

The predicted results of temperature were not so much affected by using various values of CFLC number, TLS and RADMODD. The most influence on temperature results was by the changes in turbulence intensity, RTI. The predicted results of temperature with highest degree of RTI were significant decreased near the centerline of flame (see Figure 6-3 (b)). The difference in temperature between simulation with highest RTI and lowest RTI is 250K at the centerline of flame. In simulation with high RTI, the temperature results are around 287K under-predicted comparing to temperature results reported by Tessé. In simulations with medium and low RTI, the temperature is only 52-71K lower than temperature results reported by Tessé. The RTI is an important input value for turbulent modeling. The correctly defined values of RTI are necessary for predictions of turbulent mixing process where RTI is used for calculation of turbulence kinetic energy, k.

The influence of radiation model on temperature results at radial position is shown in Figure 6-4.

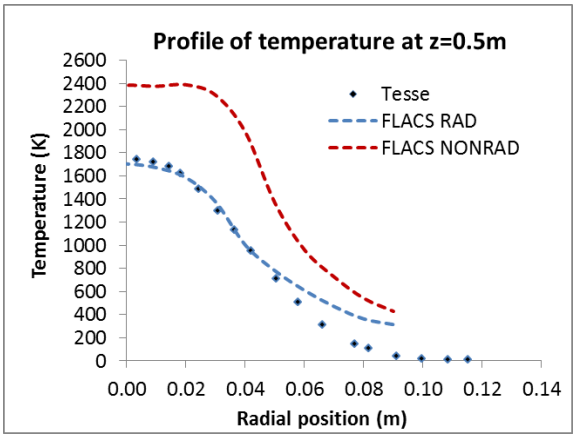

Figure 6-4 *The predicted results of temperature with radiation model and without radiation model*

The result of temperature without radiation model is drastically changed. The maximum centerline temperature computed without radiation is 642K higher than temperature results predicted by Tessé [26]. The maximum temperature computed with radiation model is 1703K, 39K lower than temperature results from simulations of Tessé. In combustion modeling, the calculation of radiation is necessary for accuracy in prediction of the flame temperature. The energy is transferred from the high temperature location to cooler surroundings by thermal radiation. This transfer of energy by radiation leads to a lower combustion temperature in the flame. In simulation without radiation model the temperature of the flame was much higher than simulation with radiation model due to negligible the radiation modeling (no heat loss by radiation).

6.2 Vertical jet flame of ethylene with D=3mm

The goal of this simulation work was to see the capability of FLACS-Fire to predict the soot volume fractions and temperature of the sooty ethylene jet flame. The temperature and soot volume fractions at different radial and axial locations of the flame were predicted using FLACS-Fire and compared with experimental measurements [32] and simulations results reported by Kleiveland [22]. The calculating domain is 0.24m×0.24m×1.220m. The total number of cells used in simulations is 41×41×67. The smallest grid cell size equals to nozzle jet diameter and uniform within the flame region. The grid cells outside the fire region were stretched towards the boundaries.

Predicted and experimental profiles of temperature and mixture fractions at the center line are shown respectively in Figure 6-5.

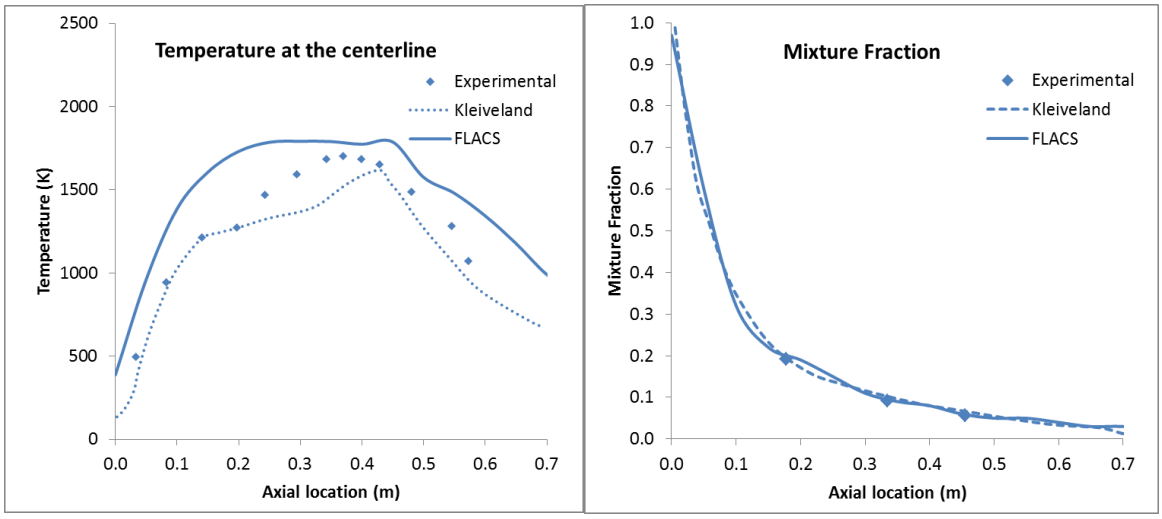

Figure 6-5 *Temperature and mixture fraction profiles at the centerline of flame*

The predicted results of temperature at the centerline of flame are over-predicted compared to experimental measurements and numerical results reported by Kleiveland. The temperature results of Kleiveland are under-predicted in comparison to measured. The mean deviation in temperature between experimental values and predicted by FLACS-Fire is 237K.

The mixture fraction at the centerline was well predicted compared to both experimental measurements and Kleiveland results.

Radial profiles of computed and measured temperature profiles at different axial locations are shown in Figure 6-6.

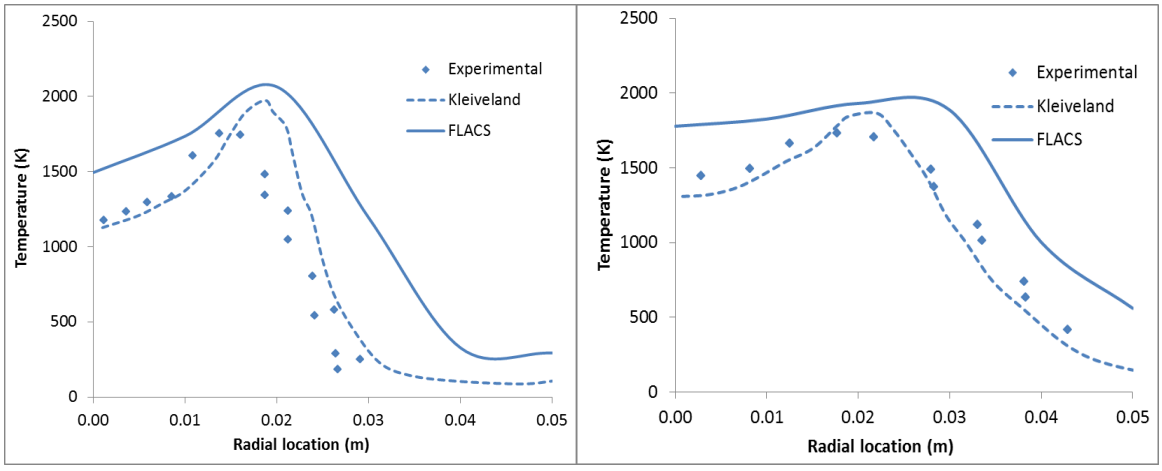

(a)Temperature at z=0.14m (b)Temperature at z=0.24m

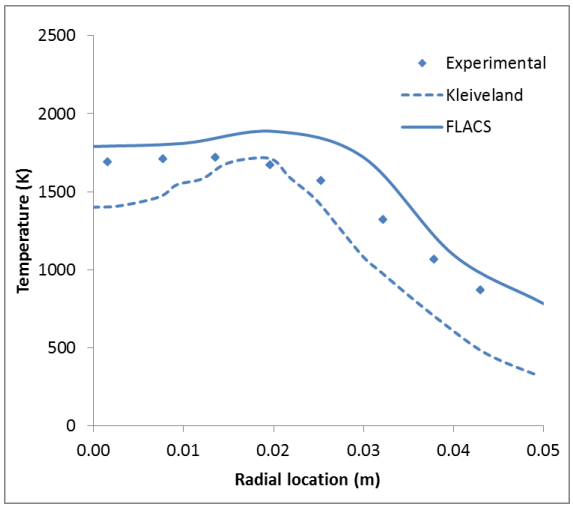

(c) Temperature at z=0.34m

Figure 6-6 *Radial profiles of temperature at different axial locations*

The predicted results of temperature are over-predicted at all flame locations compared to experimental measurements and results reported by Kleiveland. At axial location 0.34m downstream the nozzle the predicted temperatures are generally in a good agreement where the maximum discrepancies in temperature are 150K. At the outer part of the flame, the predicted temperatures decrease too rapidly.

The location of the peak temperature is shifted outwards in the simulated flame compared to the experimental measurements. The spread of the jet seems to be over-predicted in simulations.

In the combustion of ethylene the soot particles will enhance radiation from the flame and the peak of temperature is affected by the thermal radiation emitted from the soot particles. At the flame locations where soot volume fraction is high the heat loss soot is largest and leads to lower flame temperature. The experimental results showed this coupling between the soot volume fraction and temperature measurements. The peak temperature is lowest (Figure 6-6, (c)), where the soot fraction is largest (Figure 6-7, (c)).

In simulations performed by Kleiveland, the temperatures are under-predicted due to overestimation of the soot volume fractions.

The amount of soot formation at different locations can effect on the prediction of temperature. The predicted soot formation fractions are shown in Figure 6-7.

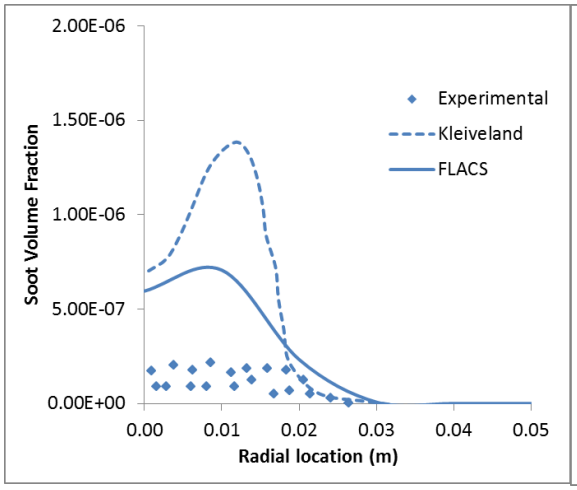

(a) Soot volume fraction at z=0.14m

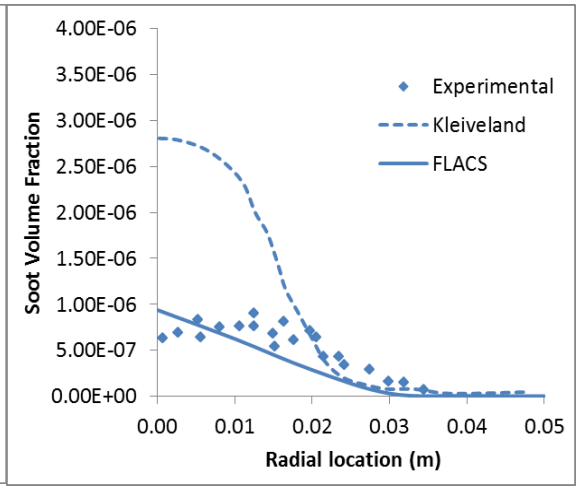

(b) Soot volume fraction at z=0.24m

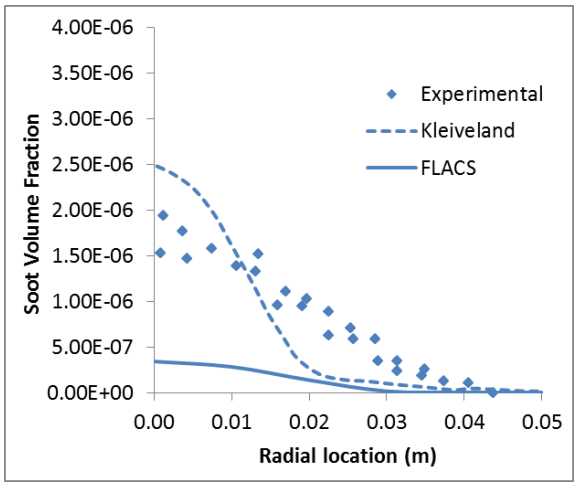

(c) Soot volume fraction at z=0.34m

Figure 6-7 *Soot volume fraction at different axial locations*

At the position z=0.14, the peak location of the soot volume fraction is not at the flame centerline and the predicted soot volume fractions fall rapid towards to the outside the centerline. The same trend was observed in temperature profiles. (See Figure 6-6 (a)). The soot volume fractions at 0.14m were over-predicated compared to experimental results but closer to experimental measurements than results reported by Kleiveland. The maximum soot volume fractions are predicted at z=0.24m. The lowest soot volume fractions predicted by FLACS-Fire are at z=0.34m, while the experimental results showed the largest soot volume fraction at the same flame region. The numerical simulations seem to predict soot earlier than the experimental results and therefor the soot reach its maximum at z=0.24m in simulations.

The ethylene flame is sooty flame. In simulations of sooty flames, both the radiation and soot modeling will influence the temperature in the flame.

The soot volume fractions are reasonable predicted compared to experimental measurements. The prediction of radiation can be affected on soot modeling. The radiation influences the temperature results.

6.3 Vertical jet flame of propane in still air

Two propane jet flames of different velocity were simulated and compared with experimental measured from Palacios et al. (2009) [27]. The results of flame length for jet velocity of 150m/s and 250m/s are shown in Figure 6-8. The finest grid size that is equal to nozzle diameter was used near the heat release source and stretched outside the boundary conditions in all three directions.

The outer boundary conditions of the flame based on the flame size from experiments using visual observation, infrared imaging or a temperature threshold. It was decided to use the temperature criterion as the flame boundary. The experimental results for propane jet fire showed that the top of the flame had the temperature 1600K [28] In this work, the temperature threshold of 1500 K has been used for the flame boundary.

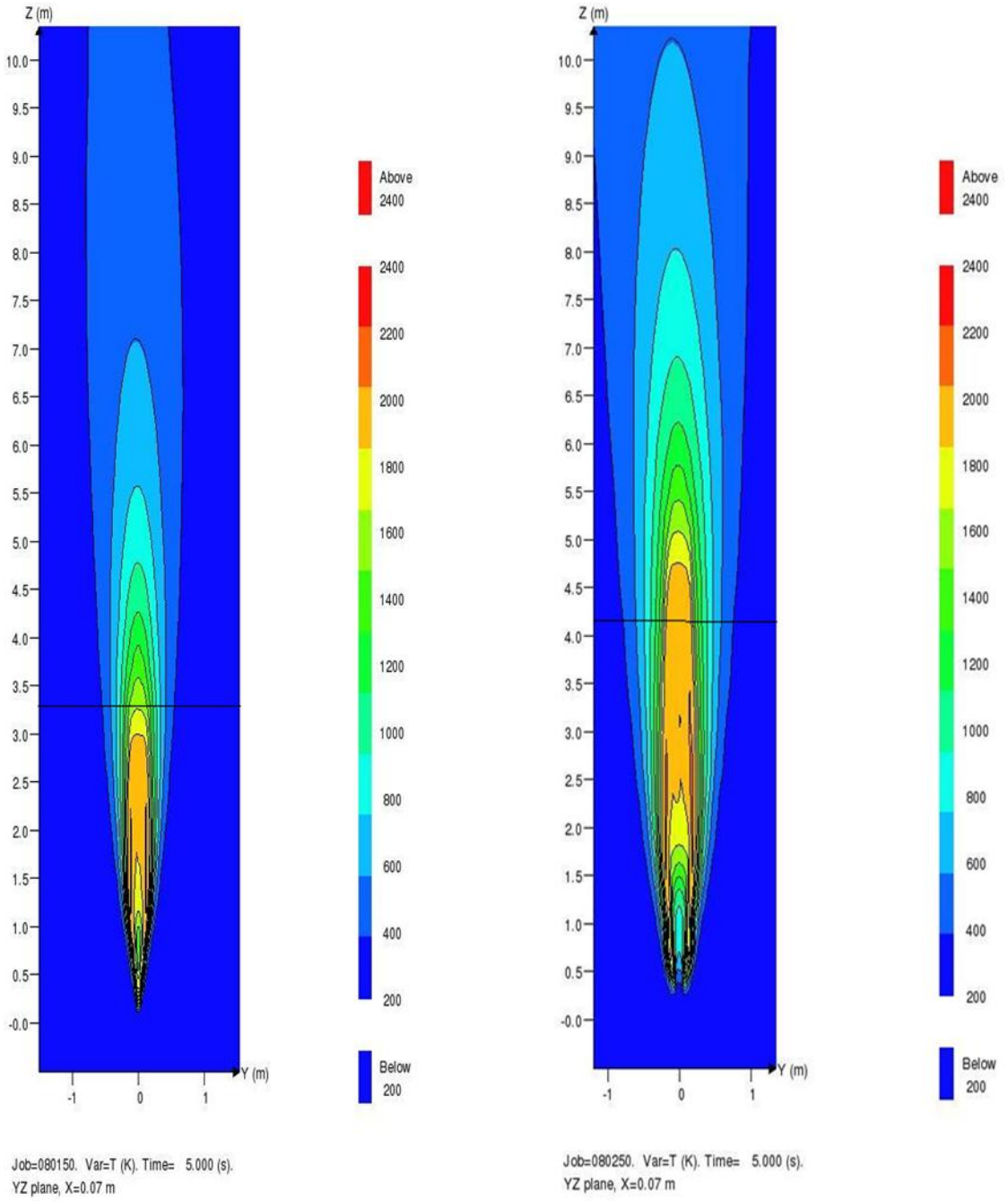

Figure 6-8*: Temperature plot of propane jet comparing 1500 K contour with experimental flame height from Palacios et al. (black line)*

The predicted flame heights were overestimated comparing with experimental data. The largest deviation of flame height has the flame of highest jet velocity, 250m/s.

In the experiments, the lift–off distance was observed in jet flames of propane and increased with increasing jet velocity. The lift-off distance of turbulent flames can be explained by extinction due to high dissipation [9] when turbulent mixing time is small.

FLACS-Fire was unable to predict the lift-off distance of flame. In all simulations, the flame is attached directly to the burner. Calculations based on the fast-chemistry assumption where the flame is during computational time not affected by local extinction. In investigation of Extinction Model in EDC performed by Torleif Weydahl et al. [34], the predicted fine-

structure time scale and dissipation of turbulent kinetic energy was influenced by assumption of chemistry. The turbulent $k-\varepsilon$ model with fast chemistry predicted larger fine-structure time scale than $k-\varepsilon$ model with detailed chemistry. When time scale for fine structures is large, the dissipation of turbulent kinetic energy is small.

The lack of the lift–off distance prediction can affect the results of simulated flame height. Nilsen [29] simulated jet flames of different velocities and his results showed a good prediction of flame heights with low velocities where the lift-off distances were smallest. The calculation of lift-off height for larger fires is important to take into account for numerical accuracy of the flame height.

Summary of the flame height results showed in Table 6-2.

Table 6-2 *The experimental and predicted results of propane flame height of different velocity*

Vertical propane jet fire with different velocities, u (m/s)	**Experimental height of flame (m)**	**Simulated height of flame (m)**	**Deviation of flame length between experimental measurements and simulated (%)**
150	3.28	3.6	10
250	4.23	5.4	28

The predicted results of temperature at centerline of the propane jet flame with velocity 250m/s compared to experimental measurements are shown in Figure 6-9.

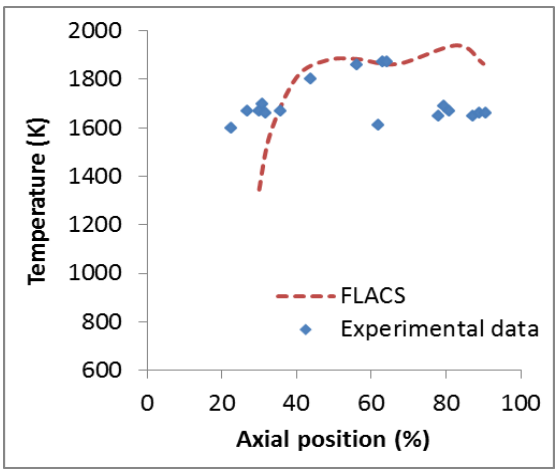

Figure 6-9 *The temperature variation along the centerline of flame*

The axial position of temperature measurements is considered in percentage and divided by radiant flame height. The predicted results of temperature in region 30%<p<70% are in good agreement with experimental values of temperature. In region p<30% the predicted temperatures are under-predicted and in region p>70 the temperatures are over-predicted. The maximum experimental temperature is 1900K at region p=60%. The maximum predicted temperature is 1940K at region p=80%.

6.4 Simulations of pool fires

Two experimental sets of heptane pool fire were modeled using FLACS-Fire: the experiment performed by Lars [31] where diameter of pool fire is 0.5m and experiment of heptane pool fire with diameter of 0.3m performed by Chih-Hung et al. [30].

6.4.1 Heptane pool fire of D=0.3m

Evaporation of liquid was modeled by 16 jet nozzles where each area of 0.00442m^2. The total mass flow rate measured from experiment was 0.00145kg/s. In simulations, the mass flow rate was distributed over 16 jet nozzles. All jet nozzles had z-direction.

The grid cell size was uniform (0.08m) over the domain, as shown in Figure 6-10. The total number of grid cells is 24×24×32.

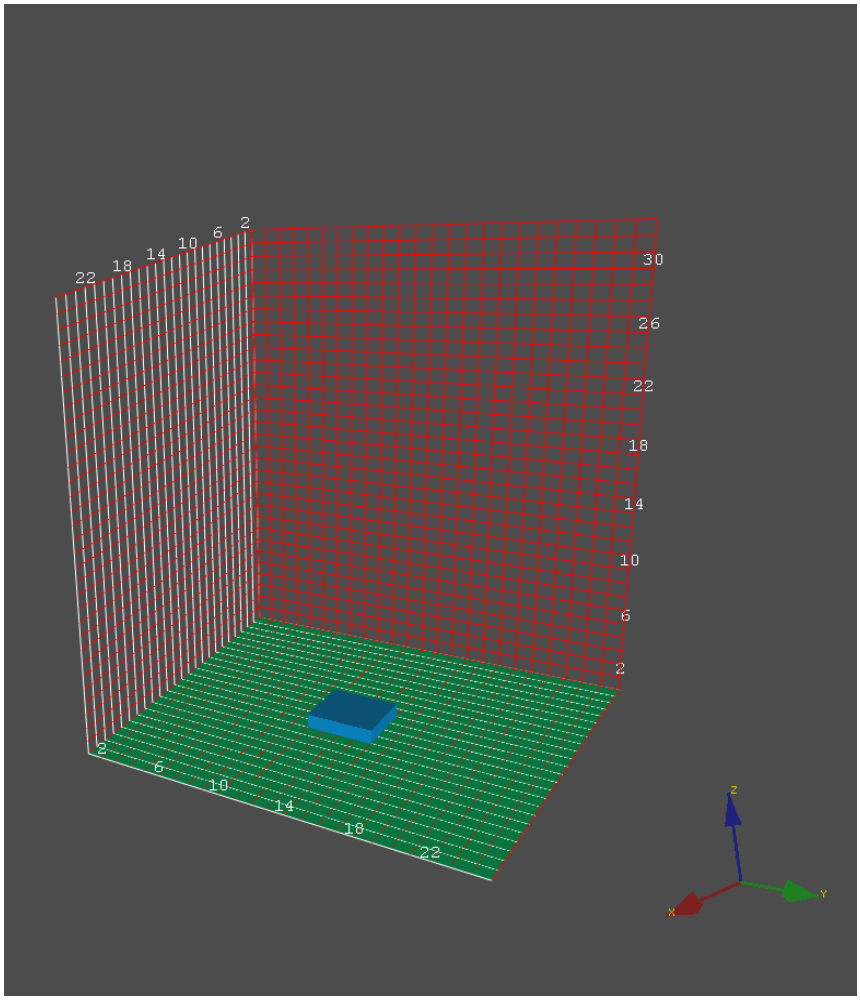

Figure 6-10 *Computed domain for heptane pool fire of D=0.3m*

The flame height and shape can be distinguished using different grids. Chin-Hung Lin at el. [30] showed the effect of the grid resolution, as presented in Figure 6-11.

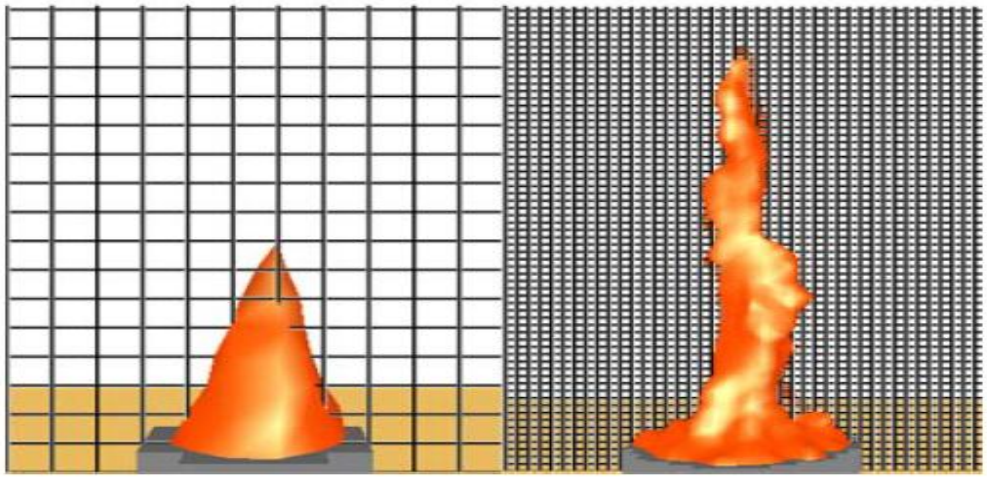

(a) Coarse grid resolution (b) Fine grid resolution

Figure 6-11 *The flame height and shape predicted by FDS with coarse grid (a) and fine grid resolutions (b)[30]*

The predicted flame height and shape of heptane pool flame using FLACS-Fire is presented in Figure 6-12.

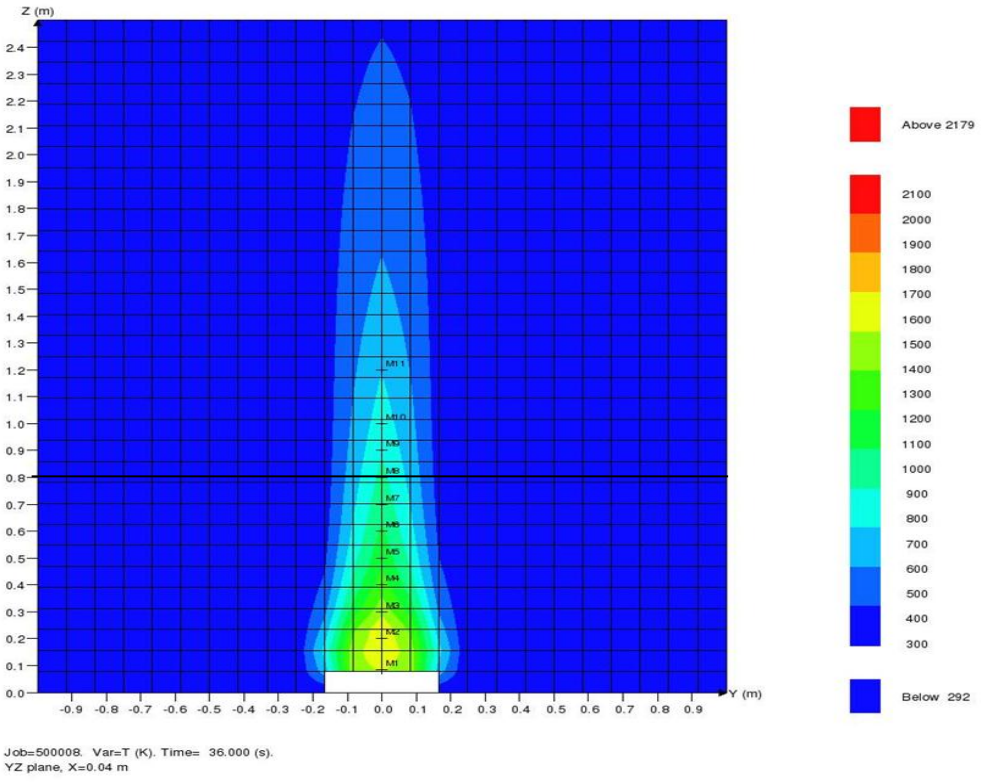

Figure 6-12 *The flame height predicted by FLACS-Fire with temperature contour 700K comparing to the flame height based on Heskestad´s correlation (black line)*

The simulated flame height based on temperature threshold. The experimental results showed that the top of the flame had the temperature 746K [30]. Therefore, the temperature threshold of 700K was used for the flame boundary.

Summary, the results of flame heights are presented in the Table 6-3.

Table 6-3 *The results of the flame heights of heptane pool flame predicted by FLACS-Fire in comparison to results from FDS and the flame height calculated by Heskestad´s correlation*

FLACS-Fire	FDS	Heskestad
1.2m	0.92m	0.91m

The results of predicted flame heights with fine grid cell-size from Lin work were in good agreement with the flame height calculated using Heskestad´s correlation [35]. In simulations performed by FLACS-Fire, the flame height was over-predicted.

The experimental and predicted results of temperature at the centerline of flame are shown in Figure 6-13

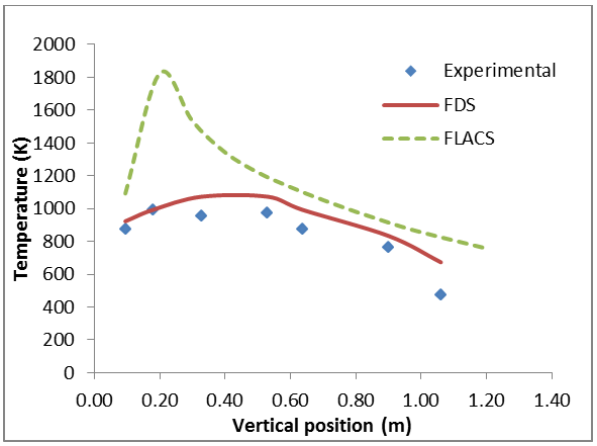

Figure 6-13 *Flame temperature at the centerline.*

The numerical results of temperature performed by FLACS-Fire and FDS codes are overestimated compared to experimental measurements. The results of temperature reported by FDS are in closer agreement with experimental measurements than simulation results performed by FLACS. At the lower part of flame, the plot of temperature increases rapid and reaches the maximum of temperature 1825K at z=0.2m. The peak of temperature in the experiment is 993K at the same location. The predicted top of temperature could be due to the lack of heat feedback effect prediction in FLACS-Fire. FLACS-Fire cannot predict the radiation from the flame to the surface of the fuel. According to Drysdale book, the radiation becomes increasingly dominant in the flames above 400℃ [7]. At the upper part of the flame the prediction of the temperature is closer to numerical results of FDS and measured.

In pool fires, the buoyancy effect has great importance for the air entrainment, the flame plume width, temperature, velocity, combustion and etc. Therefore, the accuracy of numerical simulations is largely dependent on the consideration of buoyancy effect.

The overestimation of numerical results can be related to prediction of buoyancy effect in the flame. The standard $k-\varepsilon$ model is known for to over-predict the velocities and temperatures at the centerline of the flame plume due to the lack of the buoyancy effect prediction [36].

6.4.2 Heptane pool fire of D=0.5m

Evaporation of liquid was modeled by 25 jet nozzles where each nozzle has area of $0.00785m^2$. The pool fire is presented with 25 jet nozzles for to fit a defined grid cell size. The total mass flow rate (46.4 g/s) was distributed over 25 jet nozzles. It was decided to use the combination of vertical (z) and horizontal (x, -x, y, -y) leak directions. According to simulations performed by Lars [31] the best results were presented by leak with combined xyz directions.

The size of grid-cell within the flame domain is 0.1m. Outside the fire region the grid cells are stretched towards boundaries. The total used number of grid cells in simulation is 45×45×38. The calculation domain is $6×6×4.5m^3$ and illustrated in Figure 6-14

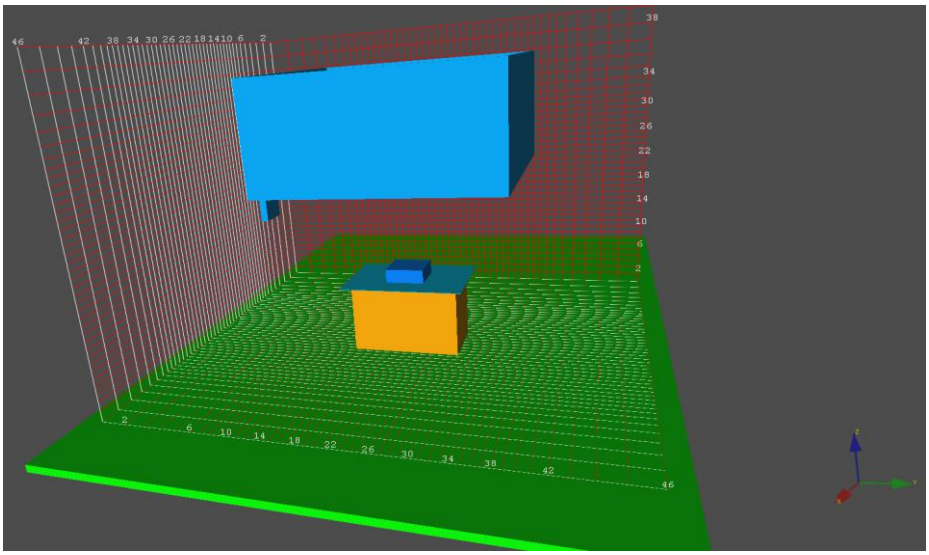

Figure 6-14 *Computed domain for heptane poo fire of D=0.5m.*

In simulation with CFLC number of 20, the temperature results along the flame centerline fluctuated (Appendix A). It was decided to perform simulation with reduced CFLC number, which value was equal 10 (Appendix B). The results of predicted temperature from simulation with CFLC number equals 10 and experimental measurements are presented in Figure 6-15.

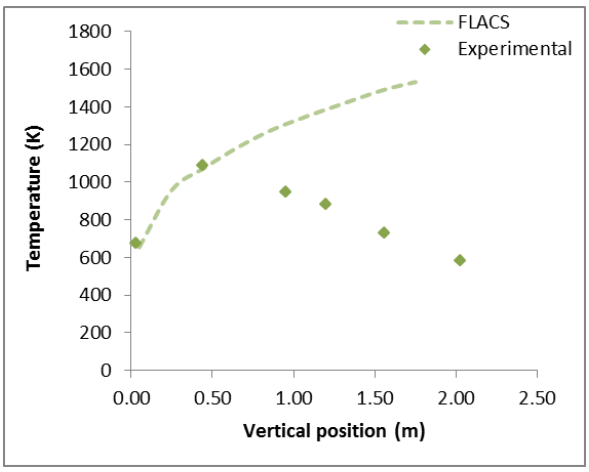

Figure 6-15 *The temperature results at the centerline of flame*

At vertical position of the flame under 0.5m the flame temperature was in good agreement with experimental measurements. The results of temperature were over-predicted compared to experimental measurements at the upper part of the flame. Deviation in temperature results increased with distance from the base of flame. From the plot of temperature as function of time the temperature values at upper part of the flame fluctuated more than temperatures at the lower part of flame. The simulated flame height was higher than experimental flame height. The large part of flame was inside the exhaust hood where the temperature is influenced by conduction and radiation.

7 Conclusion

The objective of the present work has been validation of the FLACS-Fire code by modeling turbulent diffusion flames of free burning jet fires and pool fires. The combustion model used was the Magnussens´s Eddy Dissipation Concept (EDC). The predicted results were compared to experimental values and to numerical results from other authors. The EDC combustion model was used in combination with the Discrete Transfer Radiation model and Mgnussen´s soot model. Turbulence was modeled using the $k-\varepsilon$ turbulence model. The fluid flow is solved numerically through the Favre-averaged conservation equation of mass, momentum and energy in three-dimensional geometry.

The results showed that the Eddy Dissipation Concept in FLACS-Fire was capable to reproduce the nature of turbulent jet flames. The profiles of temperature in jet flames are predicted within acceptable accuracy. Simulations done without a radiation model showed the importance of radiation since temperature results were strongly over-predicted. The volume soot fractions predicted by FLACS-Fire are close to experimental results. Prediction of soot concentration is important for accuracy of radiation.

The flame lengths were over-predicted and high momentum resulted in higher deviation. The FLACS-Fire simulations are unable to predict lift-off distance of jet flames since the extinction criteria in the EDC model is error for calculation of extinction in the jet. The improvement of the extinction models is needed to solve the problems related to predictions of lift-off distance in FLACS-Fire.

The temperature results were over-predicted in pool fires. The calculation of heat feedback effect from the fire to surface of pool is not included, so the evaporation rate from the pool will not be influenced by variation of radiation.

In summary, the main findings from the validation of FLACS-Fire:

- High grid resolution within the flame domain seems to be important for good numerical representation of the flame. Simulations of jet flames with high grid resolution improved the prediction of temperature results.
- The predicted temperature of jet flames was in good agreement with the experimental results.
- FLACS-Fire is unable to predict lift-off distance of jet flames due to no local flame extinction.
- The predicted temperatures are strongly influenced on radiation model. The predicted temperatures without radiation model lead to much higher temperature compared to experimental values. The inclusion of radiation model in numerical simulations is important for accuracy of results. The implemented radiation model in FLACS-Fire is capable to handle jet flames.
- In simulations of pool fires, the temperatures at the centerline were over-predicted compared to experimental measurements. The FLACS-Fire is unable to predict heat feedback effect which is driving force for combustion process in the pool flame. Therefore, the nature of the pool flame in numerical simulations, where the evaporation rate of fuel is represented with many nozzles, was not equivalent to real pool fire.

8 Recommendations for further work

The FLACS-Fire is under development and the fire model improves continuously. Validation of model is necessary process before FLACS-Fire can be used with confidence in the risk assessment of different flame scenarios.

Suggestions for further work are listed below:

- Modeling of the pool fire using pool model with evaporation due to radiation from flame to pool surface instead of jets leaks.
- Modeling and validation of large scale flames
- Modeling of impinging flames
- Modeling of confined fires
- Use of buoyancy modified $k - \varepsilon$ model in simulations of pool fires
- Investigate the effect of soot modeling in pool fires.
- Use of reaction schemes (reduced mechanisms) involving detailed reactions with more species
- Use of improved extinction model in simulations of jet fires to include lift-off in calculation.

References

1. Vílchez, J.A., et al., *Historical analysis of accidents in chemical plants and in the transportation of hazardous materials.* Journal of Loss Prevention in the Process Industries, 1995. **8**(2): p. 87-96.
2. P.Lees, F., *Loss Prevention in the process industries. Hazard identification, assessment and control.* 1996. **2**.
3. John D. Anderseon, J., *Computational Fluid Dynamics.* 1995.
4. Kevin, M.e.a., *Fire Dynamics Simulator (FDS) Manual.* 2010.
5. Bjørn E.Vembe, N.I.L., Jens K. Holen and Bjørn F. Magnussen, *Kameleon FireEx, A Simulator for Gas Dispersion and Fires.* 1998.
6. Simcox, S., N.S. Wilkes, and I.P. Jones, *Computer simulation of the flows of hot gases from the fire at King's Cross Underground station.* Fire Safety Journal, 1992. **18**(1): p. 49-73.
7. Drysdale, D., *An introduction to fire dynamics.* 1999: p. 8.
8. Centre, T.F.S.A., *Fire tetrahedron.* p. http://www.firesafe.org.uk/information-about-the-fire-triangletetrahedron-and-combustion/.
9. J.Warnats, U.M., R.W. Dibble, *Combustion Physical and Chemical Fundamentals, Modeling and Simulation, Experiments, Pollutant Formation*. Vol. 4. 2006.
10. eNotes, *Electromagnetic spectrum.* p. http://www.enotes.com/topic/Electromagnetic_spectrum.
11. Hottel, H.C. and W.R. Hawthorne, *Diffusion in laminar flame jets.* Symposium on Combustion and Flame, and Explosion Phenomena, 1949. **3**(1): p. 254-266.
12. McCaffrey, B.J., *Purely Buoyant Diffusion Flames: Some Experimental Results.* 1979.
13. Guan Heng Yeoh, K.K.Y., *Computational Fluid Dynamics in Fire Engineering*2009. 90.
14. GexCon, A., *FLACS v9.1 User`s Manual* 2011.
15. Olav R. Hansen, D.M., Kees van Wingerden and Trygve Skjold, *FLACS-Fire: Modelling and QRA Methodology.* 2012.
16. Ertesvåg, I.S., *Turbulent Strøyming og Forbrenning.* 2000: p. 48-56.
17. Launder, B.E. and D.B. Spalding, *The numerical computation of turbulent flows.* Computer Methods in Applied Mechanics and Engineering, 1974. **3**(2): p. 269-289.
18. Spalding, D.B., *Mixing and chemical reaction in steady confined turbulent flames.* Symposium (International) on Combustion, 1971. **13**(1): p. 649-657.
19. Magnussen, B.F. and B.H. Hjertager, *On mathematical modeling of turbulent combustion with special emphasis on soot formation and combustion.* Symposium (International) on Combustion, 1977. **16**(1): p. 719-729.
20. Magnussen, B.F., *THE EDDY DISSIPATION CONCEPT A BRIDGE BETWEEN SCIENCE AND TECHNOLOGY.* 2005.
21. Ertesvag, I.S. and B.F. Magnussen, *The eddy dissipation turbulence energy cascade model.* Combustion Science and Technology, 2000. **159**: p. 213-235.
22. Kleiveland, R.N., *Modelling of Soot Formation and Oxidation in Turbulent Diffusion Flames.* 2005.
23. Muthusamy, D., *Implementation of Radiative Transfer Calculations in the FLACS.* 2012.
24. Yin, C., et al., *New Weighted Sum of Gray Gases Model Applicable to Computational Fluid Dynamics (CFD) Modeling of Oxy–Fuel Combustion: Derivation, Validation, and Implementation.* Energy & Fuels, 2010. **24**(12): p. 6275-6282.
25. Joyeux, A.C.a.D., *Temperature and Soot Volume Fraction in Turbulent Diffusion Flames:Measurements of Mean and Fluctuating Values.* 1994.

26. Tessé, L., F. Dupoirieux, and J. Taine, *Monte Carlo modeling of radiative transfer in a turbulent sooty flame.* International Journal of Heat and Mass Transfer, 2004. **47**(3): p. 555-572.
27. Palacios, A., M. Muñoz, and J. Casal, *Jet fires: An experimental study of the main geometrical features of the flame in subsonic and sonic regimes.* AIChE Journal, 2009. **55**(1): p. 256-263.
28. Gómez-Mares, M., M. Muñoz, and J. Casal, *Axial temperature distribution in vertical jet fires.* Journal of Hazardous Materials, 2009. **172**(1): p. 54-60.
29. Nilsen, C., *Jet diffusion flames in FLACS Fire.* 2010.
30. Chin-Hung Lin, Y.-M.F., Wen-Shieng Hsu and Bau-Shei Pei, *Investigation on the Characteristics of Radiative Heat Transfer in Liquid Pool Fires.* Department of Engineering and System Science, National Tsing Hua University, 2008. **101,Sec.2**.
31. Skarsbø, L.R., *An Experimental Study of Pool Fires and Validation of Different CFD Fire Models.* 2011.
32. Kent, J.H., *Turbulent diffusion flame sooting—Relationship to smoke-point tests.* Combustion and Flame, 1987. **67**(3): p. 223-233.
33. Palacios, A. and J. Casal, *Assessment of the shape of vertical jet fires.* Fuel, 2011. **90**(2): p. 824-833.
34. Torleif Weydahl, T.M.a.I.S.E., *Investigation of the Eddy Dissiaption Extinction Model for Turbulent-Flame Simualations with Chemical Kinetics.* 2001: p. 1-5.
35. Heskestad, G., *Luminous heights of turbulent diffusion flames.* Fire Safety Journal, 1983. **5**(2): p. 103-108.
36. Yan, Z. and G. Holmstedt, *A two-equation turbulence model and its application to a buoyant diffusion flame.* International Journal of Heat and Mass Transfer, 1999. **42**(7): p. 1305-1315.

Appendix A-Plot of temperature as function of time, CFLC=20

P1-P9 are measured monitor points of temperature from lower part of flame (P1) to upper part (P9).

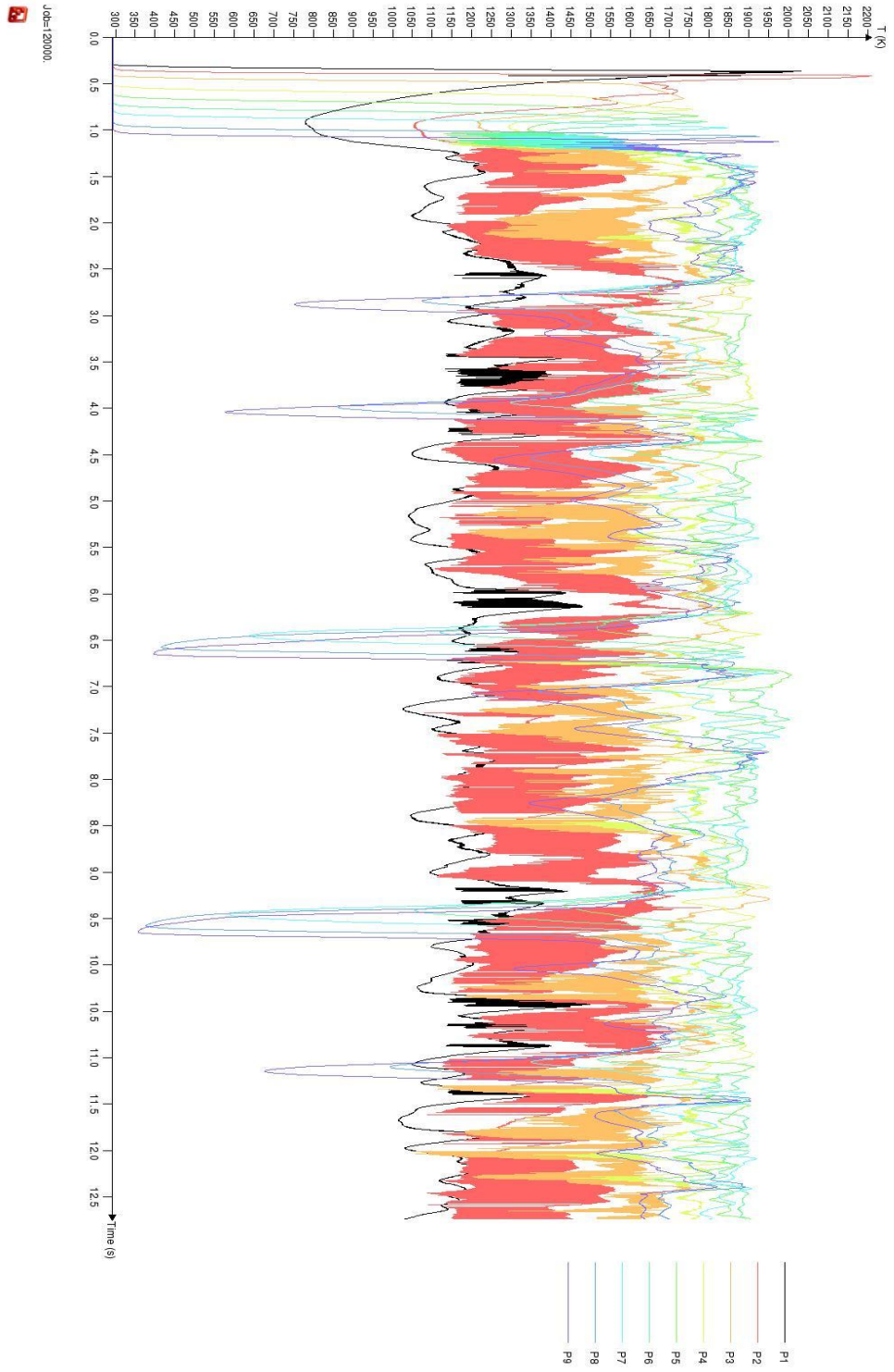

Appendix B-Plot of temperature as function of time, CFLC=10